

Set-Theoretic Estimation of Hybrid System Configurations

Emmanuel Benazera and Louise Travé-Massuyès, *Senior Member, IEEE*

Abstract—Hybrid systems serve as a powerful modeling paradigm for representing complex continuous controlled systems that exhibit discrete switches in their dynamics. The system and the models of the system are nondeterministic due to operation in uncertain environment. Bayesian belief update approaches to stochastic hybrid system state estimation face a blow up in the number of state estimates. Therefore, most popular techniques try to maintain an approximation of the true belief state by either sampling or maintaining a limited number of trajectories. These limitations can be avoided by using bounded intervals to represent the state uncertainty. This alternative leads to splitting the continuous state space into a finite set of possibly overlapping geometrical regions that together with the system modes form configurations of the hybrid system. As a consequence, the true system state can be captured by a finite number of hybrid configurations. A set of dedicated algorithms that can efficiently compute these configurations is detailed. Results are presented on two systems of the hybrid system literature.

Index Terms—Configurations, estimation, hybrid systems, numerically bounded uncertainty.

I. INTRODUCTION

THIS paper is concerned with the state estimation of plants that are modeled as hybrid systems with uncertainty. It is targeted at the monitoring and diagnosis of these plants. Most of the modern controlled systems exhibit continuous dynamics with abrupt switches. These systems can be modeled with a mixture of discrete and continuous variables. The discrete dynamics evolve according to the switches that are represented by transitions among a set of discrete modes. The behavioral continuous dynamics are modeled within each mode, often by a set of discrete-time equations. In general, the full hybrid state remains only partially observable. Depending on the level of abstraction of the model, or because of physical or design impediments, some switches cannot directly be observed neither. The estimation of the hybrid state is the operation that reconstructs the whole hybrid state based on a stream of measurements and the knowledge of the hybrid model. This is also known as hybrid state filtering, and the module that performs this operation is called a filter. Most plants operate

in uncertain environments and are not accurately known due to the presence of sensor and process uncertainties. As a consequence, transitions among modes may be nondeterministic, and continuous behavioral models may embed a representation of instrumentation and process uncertainties. It follows that modern filtering algorithms must cope with uncertainty. Probabilities and bounded sets are two main representations of uncertainty.

State estimation of hybrid systems has received increased attention in the last decade or so. However, while the systems are hybrid in nature, a first set of methods and algorithms for hybrid state estimation has remained close to continuous state estimation techniques [1]–[3]. Another cluster of approaches has mixed a heterogeneous set of techniques for continuous state estimation with qualitative reasoning [4]–[8]. Another set is formed with particle filtering methods whose focus is on the sampling of discrete transitions [9]–[11]. This group of filters has emerged as the set of most popular techniques. Basically, they apply a Bayesian belief update to stochastic hybrid systems [10]–[14]. The filter computes a posterior probability distribution function (pdf) on the continuous part of the state for each mode. Measurement likelihood w.r.t. the pdfs is used with transition probabilities to rank the possible hybrid state estimates. These methods all suffer from several weaknesses.

The main drawback is an inevitable blowup of the number of state estimates, which are also called hypotheses. It stems from the fact that the statistics that are maintained on hypotheses with the same discrete states cannot be merged without loss. The blowup is particularly intractable when the hybrid system represents faults by discrete switches that may occur at any time. Several works have explored methods for mitigating the blowup: through better use of available information by looking ahead [15] or by enumerating the first few best estimates [16]; by merging estimates [17], [18]; and hierarchical filtering [19], risk sensitive sampling [20], learning [21], forward heuristic search [14], or mixed sampling and search [22]. However, the blowup remains inevitable, and some states with low probabilities must be dropped. Unfortunately, this can lead to the loss of the true state [23].

A second problem lies in the infinite tails of the representational pdfs. In practice, the Gaussian distribution is widely used for representing the belief states due to its good statistical properties. The distribution tails are the cause of several problems by notably preventing unambiguous fault detection [24] and elimination of hypotheses. Working with truncated Gaussian pdfs [25] has been studied as an alternative, but is unattractive

Manuscript received March 21, 2008; revised July 14, 2008 and November 4, 2008. This paper was recommended by Associate Editor W. J. Wang.

The authors are with LAAS—Centre National de Recherche Scientifique (CNRS), Université de Toulouse, 31077 Toulouse Cedex 4, France (e-mail: ebenazer@laas.fr; louise@laas.fr).

Color versions of one or more of the figures in this paper are available online at <http://ieeexplore.ieee.org>.

Digital Object Identifier 10.1109/TSMCB.2009.2015280

90 due to the loss of the statistical properties, e.g., Bayes' rule does
91 not yield a truncated Gaussian.¹

92 Additionally, the stochastic modeling of faults is weak, since
93 for a good part, the modeled faults have never been observed,
94 and, thus, *a priori* numerical knowledge such as probability of
95 occurrence is indicative at best. The reliability of the produced
96 results can, therefore, be questioned. Nevertheless, the literature
97 has produced a plethora of algorithms that run a recurrent and
98 rigorous Bayesian belief update on these values and that require
99 the computation of difficult integrands [26].

100 Finally, current modeling formalisms do not accept con-
101 straints that mix discrete and continuous variables. In general,
102 constraints over discrete variables apply to operational modes,
103 and a set of linear or nonlinear equations link continuous vari-
104 ables in each mode. However, in case of software systems or ab-
105 stracted continuous behavior systems, qualitative descriptions
106 are better suited [27], [28]. There is a need for constraints that
107 formally capture dependencies between variables of different
108 types. The absence of such constraints prevents a natural con-
109 nection between variables of different types and, consequently,
110 decouples variables that are strongly coupled in nature.

111 Adding up the facts, it appears that pdfs are simply badly
112 suited to the state estimation of uncertain hybrid systems with
113 fault models. Such considerations are not new even for con-
114 tinuous systems [29]. Tackling the ambiguity that plagues the
115 stochastic filters recommends a bounded representation of un-
116 certainty as adopted in set-theoretic approaches. Set-theoretic
117 state estimation of linear and nonlinear systems [30]–[33]
118 has been studied before, but not the case of hybrid systems.
119 This paper fills this gap by developing a hybrid scheme that
120 supports bounded uncertainty with interval models. A special
121 look is given at the articulation of discrete and continuous
122 dynamics in that case. Doing so aims at circumventing most of
123 the drawbacks that have been mentioned. Bounded uncertainty
124 yields several advantages compared to pdfs. First, it provides
125 guaranteed results, i.e., an enclosure of the whole set of real
126 solutions. For this reason, the use of bounded uncertainty has
127 been popular in applications to fault detection and diagnosis,
128 since it avoids false-positive detections [34]. Second, and most
129 importantly, it prevents exponential blowup in the number of
130 state estimates. The reason behind this key property is that
131 estimates with identical discrete states can be merged with no
132 loss of information, i.e., preserving completeness; although this
133 comes at a price. The recursive computation of convex bounded
134 trajectories suffers from the well-known *wrapping effect* that
135 results from the convex enclosure at each prediction step. This
136 is because the convex bounds provide an outer approximation
137 of complex geometrical shapes, and their computation is thus
138 plagued with a recursively growing error. This problem calls for
139 aggressive optimization techniques to mitigate the error growth.
140 Another well-known problem related to intervals is multiple
141 incident parameters. Specific strategies like optimization over a
142 time-sliding window may then be required [35]. Summarizing,

the computational burden of a stochastic filter comes from the
need of tracking a very high number of belief states, whereas
that of set-theoretic hybrid state estimation lies in the compu-
tation of tight bounds. However, as this paper shows, switched
systems sometimes offer a cheap way of tightening the bounds
as a side effect of their chopped dynamics.

The alternative idea proposed in this paper leads to splitting
the continuous state space into a finite set of possibly overlap-
ping geometrical regions that, together with the system modes,
form configurations of the hybrid system. As a consequence,
the true system state can be captured by a finite number
of hybrid configurations. This paper contrasts with the pure
prediction performed in reachability analysis of hybrid systems
[36]. First, because our estimator reconstructs the hybrid state
for arbitrary continuous dynamics and switching conditions.
Second, because it incrementally operates in sampled time:
discrete switches that occur between two sampled time steps
are reconstructed by our estimator.

Overall, this paper proposes a hybrid estimation method
that aims at computing an outer approximation of the hybrid
state. In Section II, this paper formalizes a hybrid modeling
scheme that naturally embeds both bounded uncertainty and
mixed discrete/continuous constraints over the hybrid state.
Based on these two ingredients, it is shown that there exists
a special form of mixed constraints that fully capture a system
hybrid configuration under uncertainty. Here, a *configuration*
is a mixed continuous/discrete constraint that characterizes the
possible hybrid states of the system at a given point in time.
Configurations are detailed in Section III. The hybrid state
estimation process is developed in Section IV. It is a matured
version of the work initiated in [37]. The experimental results
are given in Section V.

II. HYBRID SYSTEM WITH UNKNOWN BUT BOUNDED UNCERTAINTY

We represent a physical plant as a nondeterministic and
uncertain hybrid discrete-time model. This representation has
several key features that significantly differ from the existing
formalisms. First, all continuously valued variables are as-
sumed to be uncertain but numerically bounded. Second, the
formalism uses two timescales in parallel for the discrete and
continuous dynamics, respectively. This permits an unknown
but finite number of instantaneous switches in the discrete
dynamics to occur in-between two steps of the continuous
dynamics. Third, the representation does not make any par-
ticular assumption on the conditions triggering the switches,
particularly w.r.t. the continuous state of the system. Finally,
the model supports both qualitative and quantitative behavioral
representations. For this reason, our formalism is richer than
more traditional ones such as [38] and suitable for modeling
a wide range of physical components and plants. To help
the reader throughout this paper, Table I sums up the main
notations.

Definition 1 (Hybrid System): A hybrid system H is repre-
sented by a tuple

$$H = (X, E, Q, T, L, \Theta) \quad (1)$$

¹Interestingly, whenever some data or signal is discarded from a Gaussian distribution for falling below a threshold, the resulting data do obey a truncated Gaussian. Applying Bayes rule and approximating the resulting belief state with a new Gaussian increases the error recursively.

TABLE I
MAIN NOTATIONS

| | |
|---|---|
| H | hybrid system. |
| $\mathbf{x}_{c,k}$ | continuous state vector at sampled time-step k . |
| $\mathbf{y}_{c,k}$ | observable state vector at sampled time-step k . |
| $\tilde{\mathbf{y}}_{c,k}$ | observed state vector at sampled time-step k . |
| $x_{m,l}$ | system mode at logical time-step l . |
| $\mathbf{x}_{d,l}$ | discrete state vector at logical time-step l . |
| $\boldsymbol{\pi}_l = (\mathbf{x}_{m,l}, \mathbf{x}_{d,l})$ | full discrete state vector at logical time-step l . |
| $\mathbf{s}_{l,k} = (\boldsymbol{\pi}_l, \mathbf{x}_{c,k})$ | hybrid state vector at date (l, k) . |
| $\mathbf{s}_{l,k}^{(p)} = (\boldsymbol{\pi}_l^{(p)}, \mathbf{x}_{c,k}^{(p)})$ | p -th hybrid estimate at date (l, k) . |
| ϕ_i^j | partial guard of transition τ^j in continuous dimension i . |
| g_i^j | condition function that determines the Boolean value of ϕ_i^j . |
| $\tilde{\mathbf{x}}_{c,k}^j$ | positive domain: enabling region of transition τ^j in $\mathbf{x}_{c,k}$. |
| \mathbb{X}_k | conditional domain of $\mathbf{x}_{c,k}$. |
| C_k | configuration of H at sampled time-step k . |
| \mathcal{R}_{C_k} | configuration region at sampled time-step k . |
| κ_i^d | conditional vector. |
| $\nabla_{\delta k}$ | logical configuration region at sampled time-step k . |

197 where $X = \{X_d, X_c\}$ is the set of discrete and continuous
198 variables, respectively, E is the set of difference equations, Q
199 is the set of propositional formulas, \mathcal{T} is the set of transitions,
200 L is the set of continuous mapping functions associated to
201 transitions, and Θ 's are the initial variable values.

202 A. Variables and States

203 A hybrid system H abstracts the behavior of a physical
204 system through a set of functional modes. The system *mode* is
205 x_m , which has domain $\{m_1, \dots, m_{n_m}\}$. The full discrete state
206 is noted as $\boldsymbol{\pi} = (x_m, \mathbf{x}_d)$, where $\mathbf{x}_d = [x_{d1}, \dots, x_{dn_d}]^T$ is the
207 vector of other discretely valued variables used to describe qual-
208 itatively abstracted continuous behavior within modes. There-
209 fore, $X_d = \{x_m, x_{d1}, \dots, x_{dn_d}\}$. The system mode is assumed
210 not to be directly observable. \mathbf{y}_d denotes the observable subpart
211 of \mathbf{x}_d . The vector of actually observed discrete values is noted
212 as $\tilde{\mathbf{y}}_d$. The discrete input vector is noted as \mathbf{u}_d .

213 The continuous dynamics of the system are captured by the
214 continuous state vector $\mathbf{x}_c = [x_{c1}, \dots, x_{cn_c}]^T$, the observation
215 vector \mathbf{y}_c , and the continuously valued input vector \mathbf{u}_c . The
216 vector of actually observed values is noted as $\tilde{\mathbf{y}}_c$. X_c is the set
217 of all continuous variables. The continuous state is represented
218 with uncertainty in a bounded form. Thus, \mathbf{x}_c is an interval
219 vector (a box) in the continuous state space. That is, \mathbf{x}_c is
220 a closed and connected rectangular subset of \mathfrak{R}^{n_c} , or equiva-
221 lently, $\mathbf{x}_c \in IR^{n_c}$, where IR is the set of real-valued intervals.
222 The hybrid state of the system is noted as $\mathbf{s} = (\boldsymbol{\pi}, \mathbf{x}_c)$.

223 B. Time and Dynamics

224 1) *Continuous Dynamics*: Every mode is associated to a
225 unique continuous evolution model. The continuous behavior
226 of the physical system is modeled by a finite set of differ-
227 ence equations in E with uncertain but bounded parameters.
228 In each mode, x_m corresponds to a subset of discrete-time

equations of the following standard form, assuming a sampling
period T_s :

$$\mathbf{x}_{c,k} = f(\mathbf{x}_{c,k-1}, \mathbf{u}_{c,k-1}, \mathbf{w}_{c,k-1}, x_m) \quad (2)$$

$$\mathbf{y}_{c,k} = h(\mathbf{x}_{c,k}, \mathbf{v}_{c,k}, x_m) \quad (3)$$

where (2) is the state equation, (3) is the measurement equation,
 k is the discrete-time index, and $\mathbf{w}_c = [w_{c1}, \dots, w_{cn_w}]^T$ and
 $\mathbf{v}_c = [v_{c1}, \dots, v_{cn_v}]^T$ represent the process and measurement
noise vectors, respectively, and are assumed to be independent.
This uncertainty and the parameters defining f and h are
assumed to be unknown but numerically bounded. In particular,
this means that $\|\mathbf{w}_c\|_\infty \leq \epsilon_w$ and $\|\mathbf{v}_c\|_\infty \leq \epsilon_v$, where ϵ_w and ϵ_v
are known positive scalars. $\|\cdot\|_\infty$ denotes the ∞ -norm such that
 $\|\mathbf{w}_c\|_\infty = \max_i |w_{ci}|$, $i = 1, \dots, n_w$.

What we denote as the *sampled timescale* is the timeline that
is explicit in (2) and (3). The sampled time step k thus labels
the k th sampling period between continuous instants $T_s(k-1)$
and $T_s k$. $\mathbf{x}_{c,k}$ and $\mathbf{y}_{c,k}$ are the valuations of the continuous state
and the output at sampled time step k .

2) *Discrete Dynamics*: A need for an abstracted qualitative
representation of behavior was discussed in Section I. Behav-
iors that are naturally expressed by means of discrete variables,
like those of embedded software, also need to be represented.
Thus, at a discrete level, these descriptions are written in
propositional logic by a set of time-independent propositional
formulas Q over discrete variables of X_d .

What we denote as the *logical timescale* marks the sequence
of changes in the discrete dynamics of the system. With $\boldsymbol{\pi}_l =$
 $(x_{m,l}, \mathbf{x}_{d,l})$, we specify the discrete state at logical time step
 l . The switches from one mode to another are represented by
transitions. Transition τ switches H from mode $x_{m,l}$ to mode
 $x_{m,l+1}$. \mathcal{T} is the set of n_T transitions of H . Transitions are of
the following different types.

- 1) *Autonomous* transitions are triggered by conditions over
the continuous state. These conditions are referred to as
guards and noted $\phi : \mathbf{x}_c \rightarrow \{0, 1\}$. Section III conducts
an in-depth analysis of guards.
- 2) *Commanded* transitions are triggered by discrete com-
mands \mathbf{u}_d .
- 3) *Unpredictable* transitions have no guards and can trigger
anytime, for instance, fault transitions.

A transition is said to be *enabled* whenever its guard is realized.
Nondeterminism arises from the possibility of having multiple
transitions enabled simultaneously. When enabled, a transition
triggers a mode change. After a transition τ has triggered and
switched the system mode from $x_{m,l}$ to $x_{m,l+1}$, the continuous
state $\mathbf{x}_{c,k}$ becomes $l_\tau(\mathbf{x}_{c,k})$, where l_τ is denoted as the *transi-*
tion mapping function.

Transitions are assumed to be instantaneous. However, when
abstracting certain behaviors using a hybrid model, it appears
that transitions may have nonnegligible duration. The present
framework supports the triggering of a transition after a certain
delay has expired. Importantly, the transition triggering remains
instantaneous. Thus, the duration of a transition is really to
be understood as a delay, that is, a certain number d of sam-
pled time steps before an enabled transition does trigger and

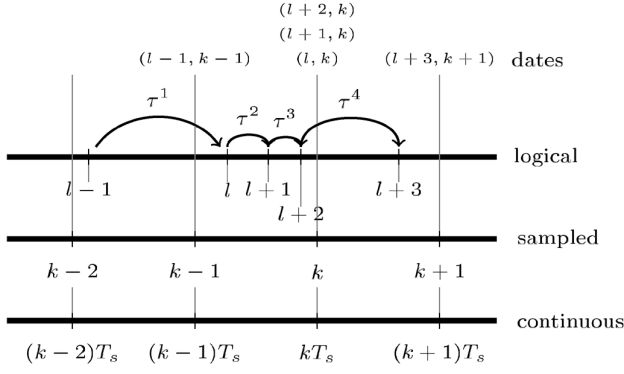


Fig. 1. Discrete and continuous parallel timescales. Transitions are instantaneous but are represented by arrows from the previous logical time step to the time step at which they trigger (e.g., τ^1 triggers at l). Dates synchronize the timescales at every sampled time point.

282 does lead to a different mode. Assuming that transition τ has
283 its autonomous guard enabled in $x_{c,k}$, it triggers d -sampled
284 time steps later, and the continuous arrival state is given by
285 $l_\tau(x_{c,k+d})$. In the rest of this paper, we assume that $d = 0$ with
286 no loss of generality.

287 3) *Discrete and Continuous Parallel Timescales*: As men-
288 tioned above, our representation uses two discretized timescales
289 in parallel on top of the continuous timescale: the sampled
290 and the logical timescales. As a consequence, changes in the
291 discrete dynamics are not assumed to take place at a particular
292 sampled time step, but can occur in-between two sampled
293 time steps. However, hybrid states need to be synchronized in
294 time. Because the sampled time evolves according to a fixed
295 sampling period T_s , the logical time is synchronized with the
296 sampled time, and not the opposite. In consequence, the logical
297 time is always associated to the first sampled time step that
298 follows a switch (see Fig. 1). Note that for this reason, an
299 instantaneous switch is always triggered after its occurrence
300 on the physical system. In this context, (l, k) is a *date* for
301 the system, and $s_{l,k}$ denotes the hybrid state at logical time
302 step l and sampled time step k . We assume that a finite but
303 unknown number of switches can occur between two sampled
304 time steps. In this case, hybrid states are indexed by dates whose
305 sampled indexes are the same, but with different logical indexes
306 (see time step k in Fig. 1). In this formulation, the execution
307 (solution trajectory) of the proposed class of hybrid systems is
308 a succession of hybrid states at established dates. The execution
309 corresponding to the succession of dates in Fig. 1 is written as

$$310 s_{l-1,k-2}, s_{l-1,k-1} \xrightarrow{\tau^1} s_{l,k} \xrightarrow{\tau^2} s_{l+1,k} \xrightarrow{\tau^3} s_{l+2,k} \xrightarrow{\tau^4} s_{l+3,k+1}.$$

311 C. Example

312 *Example 1 (Thermostat System)*: The temperature x of a
313 room is controlled by a thermostat that keeps it between
314 x^{\min} and x^{\max} degrees by switching a heater on and off.
315 The system is modeled as a hybrid system H . $X_d = \{x_m\}$
316 with domain $\{m_1 = \text{off}, m_2 = \text{on}, m_3 = \text{stuck on}, m_4 =$
317 $\text{stuck off}\}$. \mathbf{x}_c is reduced to the temperature x of the room,
318 and \mathbf{u}_c is reduced to the input u . The continuous dynam-
319 ics of the system are modeled by the first-order differential

equation $\dot{x} = D(u - x)$, where D is a multiplying factor. We
320 model $E = \{E_{m_1}, E_{m_2}, E_{m_3}, E_{m_4}\}$ with $E_{m_1} = E_{m_4}$ such
321 that $u = \bar{x}$ (i.e., the temperature outside the room), and $E_{m_2} =$
322 E_{m_3} such that $u = h$ (i.e., the heater constant whose value
323 is uncertain but bounded). In discretized form, the dynam-
324 ics are given by the following recurrent equation in stan-
325 dard form (2): $x_k = ax_{k-1} + bu_{k-1}$, with $a = 1 - DT_s$, and
326 $b = DT_s$, assuming a sampling period T_s . Q is empty, and
327 $\mathcal{T} = \{\tau^1, \tau^2, \tau^3, \tau^4\}$, where $\tau^1 : m_2 \xrightarrow{\phi^1=1 \text{ if } (x \geq x^{\max})} m_1$, $\tau^2 : m_1$
328 $\xrightarrow{\phi^2=1 \text{ if } (x \leq x^{\min})} m_2$, $\tau^3 : m_2 \xrightarrow{\phi^3=1 \text{ if } (x \geq x^{\max})} m_3$, and
329 $\tau^4 : m_1 \xrightarrow{\phi^4=1 \text{ if } (x \leq x^{\min})} m_4$. Notice that $\phi^1 = \phi^3$, and $\phi^2 =$
330 ϕ^4 . L associates the identity function to every transition. 331

III. SET-THEORETIC HYBRID CONFIGURATIONS 332

This section formalizes the concept of configuration of a 333
334 hybrid system. A canonical form of a transition guard is given.
335 It leads to the definition of a configuration as a rectangular
336 bounded region that enables a possibly empty set of transitions.
337 Another contribution is the logical abstraction of a configu-
338 ration that articulates the discrete and continuous dynamics
339 of the hybrid system. This formulation paves the way for the
340 estimation algorithms in Section IV.

A. Transition Guards 341

Commanded transition triggering is conditioned over the 342
343 discretely valued inputs \mathbf{u}_d , but these conditions are directly
344 expressed as constraints at the discrete level and do not
345 require specific processing. Autonomous transitions require
346 more attention.

Definition 2 (Autonomous Transition Guard): The guard 347
348 of an autonomous transition τ^j is noted as $\phi^j : \mathbf{x}_c =$
349 $(x_{c1}, \dots, x_{cn})^T \rightarrow \{0, 1\}$. $\phi^j(\mathbf{x}_c)$ can be expressed as a set of
350 inequalities in the canonical form given in the if condition of
351 (5). The inequalities referring to a given state variable x_{ci} define
352 the partial guard $\phi_{i_\alpha}^j(\mathbf{x}_c)$ as

$$353 \phi_{i_\alpha}^j(\mathbf{x}_c) = \bigwedge_{\alpha} \phi_{i_\alpha}^j(\mathbf{x}_c) \quad (4)$$

$$354 \phi_{i_\alpha}^j(\mathbf{x}_c) = \begin{cases} 1, & \text{if } x_{ci} \leq g_{i_\alpha}^j(x_{c1}, \dots, x_{ci-1}, x_{ci+1}, \dots, x_{cn}) \\ 0, & \text{otherwise} \end{cases} \quad (5)$$

where $g_{i_\alpha}^j : \mathbf{x}_c \rightarrow \mathfrak{R}$ is referred to as a *condition function*, and
353 \leq stands either for “ \leq ” or “ \geq .” 354

The index i_α identifies one specific condition function in 355
356 the set of condition functions referring to transition τ^j and
357 variable x_{ci} . Note that no assumption is made on the form of
358 the condition functions.² For the sake of clarity, in the rest of
359 this paper, we make two simplifying assumptions. First, we
360 assume that the set of condition functions is either empty or

²The inequality canonical form does not limit the expressiveness of the
framework. Complex inequalities can always be manipulated to be brought
back to this form, possibly by introducing new variables.

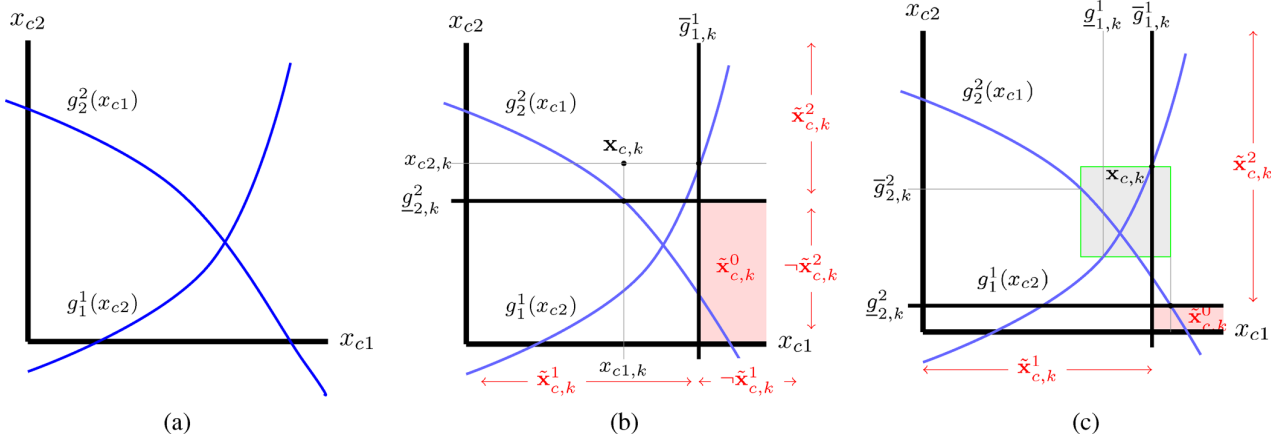


Fig. 2. Example 2: generic 2-D situation with guards $\phi_1^1 : x_{c1} \leq g_1^1(x_{c2})$ and $\phi_2^2 : x_{c2} \geq g_2^2(x_{c1})$. The positive and negative subdomains are computed from conditional functions g_1^1 and g_2^2 taken at $\mathbf{x}_{c,k}$, or at its corners when it is a box. The upper bounds to conditional domains $\bar{g}_i^j(\mathbf{x}_{c,k})$ are abbreviated as $\bar{g}_{i,k}^j$. A similar abbreviation is used for lower bounds. They yield $\mathbb{X}_k = [\tilde{\mathbf{x}}_{c,k}^0, \tilde{\mathbf{x}}_{c,k}^1, \tilde{\mathbf{x}}_{c,k}^2]$. (a) Functional representation of the guards. (b) Real-valued $\mathbf{x}_{c,k}$. (c) Uncertain $\mathbf{x}_{c,k}$ is a hyperrectangle.

361 of cardinality 1 for every x_{ci} and τ^j . In other words, there is at
 362 most one inequality referring to a variable x_{ci} associated to a
 363 partial guard ϕ_i^j . Second, we assume that $\phi_i^j(\mathbf{x}_c) = 1$ whenever
 364 the set of condition functions is empty (i.e., g_i^j is not specified).
 365 This allows us to write $\phi^j(\mathbf{x}_c) = \bigwedge_{i=1}^{n_c} \phi_i^j(\mathbf{x}_c)$.

366 Unpredictable transitions are modeled with guards such that
 367 $\phi^j = 1$, independent of \mathbf{x}_c . When the model contains guards
 368 as disjunctions of inequalities, these can be broken into guards
 369 over several transitions and modes. Admittedly, the modeling
 370 of a discrete switch as a transition whose guard is made of e
 371 disjunctions of inequalities necessitates a total of 2^e modes.
 372 τ^j is said to be enabled in the hybrid state $\mathbf{s} = (\boldsymbol{\pi}, \mathbf{x}_c)$
 373 whenever $\phi^j(\mathbf{x}_c) = 1$. When enabled, the triggering of the
 374 transition is an instantaneous transfer of the hybrid state to
 375 another state (possibly identical) at the next logical time step.
 376 This operation is detailed in Section IV along with the hybrid
 377 state estimator. The rest of this section studies the structure
 378 of the continuous space as constrained by the autonomous
 379 transition guards.

380 B. Grid of Configurations

381 At sampled time step k , the evaluation of transition guards
 382 against a continuous vector $\mathbf{x}_{c,k}$ is done through the evaluation
 383 of the condition functions $g_i^j(\mathbf{x}_{c,k})$. Each inequality referring
 384 to a condition function indeed splits the domain of $\mathbf{x}_{c,k}$ in two
 385 subdomains.

- 386 1) $\tilde{\mathbf{x}}_{c,k}^j = \{(x_{c1}, \dots, x_{cn_c})^T | \phi^j(\mathbf{x}_{c,k}) = 1\}$: The region
 387 that satisfies the inequalities or *positive* subdomain. $\tilde{\mathbf{x}}_{c,k}^j$
 388 denotes the region in which transition τ^j is enabled at
 389 sampled time step k .
- 390 2) The region that does not satisfy the inequality or negative
 391 subdomain, which is noted as $\neg\tilde{\mathbf{x}}_{c,k}^j = \mathfrak{R}^{n_c} - \tilde{\mathbf{x}}_{c,k}^j$ (com-
 392plementary set of $\tilde{\mathbf{x}}_{c,k}^j$).

393 As $\mathbf{x}_{c,k}$ defines a box in \mathfrak{R}^{n_c} , the values of $g_i^j(\mathbf{x}_{c,k})$ are bounded
 394 intervals of the form $[g_{i,k}^j(\mathbf{x}_{c,k}), \bar{g}_{i,k}^j(\mathbf{x}_{c,k})]$. Thus, $\tilde{\mathbf{x}}_{c,k}^j$ and $\neg\tilde{\mathbf{x}}_{c,k}^j$

are interval vectors of dimension n_c , the scalar bounds of which
 395 take value $g_{i,k}^j(\mathbf{x}_{c,k})$, $\bar{g}_{i,k}^j(\mathbf{x}_{c,k})$, $-\infty$, or $+\infty$. Considering all
 396 the autonomous transitions, this formulation leads to splitting
 397 the continuous space into several overlapping subregions. The
 398 set of positive and negative subdomains for $\mathbf{x}_{c,k}$ for all the
 399 autonomous transitions is used to build what we refer to as the
 400 conditional domain of $\mathbf{x}_{c,k}$.

Definition 3 (Conditional Domain): Given a hybrid system
 402 H , the conditional domain of $\mathbf{x}_{c,k}$ at k is given by $\mathbb{X}_k =$
 403 $[\tilde{\mathbf{x}}_{c,k}^0, \tilde{\mathbf{x}}_{c,k}^1, \dots, \tilde{\mathbf{x}}_{c,k}^T]$, where we have the following:

- 404 1) $\tilde{\mathbf{x}}_{c,k}^j$ is the positive subdomain for every transition τ^j ,
 405 $j = 1, \dots, n_T$ of H ;
 406
- 407 2) $\tilde{\mathbf{x}}_{c,k}^0 = \bigcap_{j=1}^{n_T} (\neg\tilde{\mathbf{x}}_{c,k}^j)$ is the region that satisfies no partial
 408 guard.

Example 1 (Continued): The model has two guards over four
 409 transitions. Guards depend on temperature $\mathbf{x}_c = x$ only. Then,
 410 $\mathbb{X}_k = [\tilde{x}_k^0, \tilde{x}_k^1, \tilde{x}_k^2, \tilde{x}_k^3, \tilde{x}_k^4]$ with $\tilde{x}_k^0 = [x^{\min}, x^{\max}]$, $\tilde{x}_k^1 = \tilde{x}_k^3 =$
 411 $]-\infty, x^{\min}]$, and $\tilde{x}_k^2 = \tilde{x}_k^4 = [x^{\max}, +\infty[$.

Example 2: Consider a hybrid system H with x_m taking
 413 its value in domain $\{m_1, m_2, m_3\}$, $\mathbf{x}_c = [x_{c1}, x_{c2}]^T$, and $\mathcal{T} =$
 414 $\{\tau^1, \tau^2\}$ with $\tau^1 : m_1 \xrightarrow{\phi^1} m_2$, $\tau^2 : m_1 \xrightarrow{\phi^2} m_3$, and $\phi^1 = \phi_1^1 :$
 415 $\begin{cases} 1, & \text{if } x_{c1} \leq g_1^1(x_{c2}) \\ 0, & \text{otherwise} \end{cases}$, $\phi^2 = \phi_2^2 : \begin{cases} 1, & \text{if } x_{c2} \geq g_2^2(x_{c1}) \\ 0, & \text{otherwise} \end{cases}$.

Initially, H is in mode m_1 . Fig. 2 shows the conditional
 417 domain for this generic 2-D example in two situations: when
 418 $\mathbf{x}_{c,k}$ is real valued and when $\mathbf{x}_{c,k}$ is a box. In both cases, the
 419 conditional domain is given by

$$\begin{aligned} \mathbb{X}_k &= [\tilde{\mathbf{x}}_{c,k}^0, \tilde{\mathbf{x}}_{c,k}^1, \tilde{\mathbf{x}}_{c,k}^2] = \begin{bmatrix} \tilde{x}_{c1,k}^0 & \tilde{x}_{c1,k}^1 & \tilde{x}_{c1,k}^2 \\ \tilde{x}_{c2,k}^0 & \tilde{x}_{c2,k}^1 & \tilde{x}_{c2,k}^2 \end{bmatrix} \\ &= \begin{bmatrix} [\bar{g}_{1,k}^1, +\infty[&]-\infty, \bar{g}_{1,k}^1] &]-\infty, +\infty[\\]-\infty, g_{2,k}^2[&]-\infty, +\infty[& [g_{2,k}^2, +\infty[\end{bmatrix} \end{aligned}$$

where $g_{i,k}^j$ abbreviates $g_i^j(\mathbf{x}_{c,k})$. Note that when $\mathbf{x}_{c,k}$ is real
 421 valued, $g_{i,k}^j = \bar{g}_{i,k}^j$.

423 \mathbb{X}_k concretizes the split³ of the continuous space defined by
 424 the autonomous transition guards at time step k . Note that \mathbb{X}_k
 425 evolves and is reshaped according to the continuous state vector
 426 at each time step. Geometrically, the bounds of $\tilde{\mathbf{x}}_{c,k}^j$ define
 427 edges that split the continuous state space into overlapping
 428 volumes shaped by boxes. Later developments require the
 429 definition of the bounds of these boxes. The lower bound of
 430 \mathbb{X}_k is written as $\underline{\mathbb{X}}_k$, and the upper bound is written as $\overline{\mathbb{X}}_k$.
 431 Every combination of elements of \mathbb{X}_k corresponds to a sub-
 432 region of the continuous state space in which some transitions
 433 are enabled and some are not. These regions are in the form
 434 of bounded boxes that support the concept of *configuration* of
 435 the hybrid system H . A configuration corresponds to a possi-
 436 ble situation of the hybrid system in terms of simultaneously
 437 enabled and nonenabled transitions. Due to the boxed shape
 438 of the regions, the set of all configurations is organized in a
 439 grid that evolves with time, which is dubbed as the *grid* of
 440 *configurations*.

441 **Definition 4 (Configuration):** A configuration \mathcal{C}_k of the hy-
 442 brid system H at time step k is defined as follows.

- 443 1) A *configuration region* $\mathbf{r}_{\mathcal{C}_k}$ that is a box in the continuous
 444 state space that confines a region that simultaneously
 445 enables a possibly empty subset of transitions of \mathcal{T} .
- 446 2) A *configuration function* $\delta_{\mathcal{C}_k}$ that is a Boolean function
 447 that tells whether there exist points of the continuous state
 448 $\mathbf{x}_{c,k}$ that belong to the configuration region or not.
- 449 3) A *configuration-enabling set* $\mathcal{T}_{\mathcal{C}_k}^e$ that indicates which
 450 transition(s) is (are) enabled in the configuration region.

451 A configuration \mathcal{C}_k is hence defined by a tuple $(\mathbf{r}_{\mathcal{C}_k}, \delta_{\mathcal{C}_k}, \mathcal{T}_{\mathcal{C}_k}^e)$.

452 **Definition 5 (Configuration Region):** At time step k and for
 453 continuous vector $\mathbf{x}_{c,k}$, consider for every $i = 1, \dots, n_c$ a unit⁴
 454 vector β_i of size $n_T + 1$. $\{\beta_1, \dots, \beta_{n_c}\}$ form a set of pro-
 455 jection vectors that extract a combination of transition partial
 456 guards, one per continuous dimension. Then, a configuration
 457 region is the volume defined by

$$\mathbf{r}_{\mathcal{C}_k} = [\underline{\mathbb{X}}_{k,[1,]} \beta_1, \dots, \underline{\mathbb{X}}_{k,[n_c,]} \beta_{n_c}]^T \quad (6)$$

458 where $\underline{\mathbb{X}}_{k,[i,]}$ yields the i th line of matrix $\underline{\mathbb{X}}_k$.

459 Using bounds of the conditional domain, we write the con-
 460 figuration region's frontier as the lowermost and uppermost
 461 vertices of the region's hyperrectangle. They are given by

$$\begin{aligned} \bar{\mathbf{r}}_{\mathcal{C}_k} &= [\underline{\mathbb{X}}_{k,[1,]} \beta_1, \dots, \underline{\mathbb{X}}_{k,[n_c,]} \beta_{n_c}]^T \\ &\cup [\overline{\mathbb{X}}_{k,[1,]} \beta_1, \dots, \overline{\mathbb{X}}_{k,[n_c,]} \beta_{n_c}]^T. \end{aligned} \quad (7)$$

462 Different configuration regions may overlap. A consequence is
 463 that some configurations may be subsumed by some set of other
 464 configurations and then be left aside. In example 2, any region
 465 obtained with $\beta_1 = \begin{bmatrix} 0 \\ 0 \\ 1 \end{bmatrix}$ and/or $\beta_2 = \begin{bmatrix} 0 \\ 1 \\ 0 \end{bmatrix}$ is subsumed by
 466 regions obtained with other vectors. By extension, we say that
 467 a configuration \mathcal{C}_i is subsumed by a configuration \mathcal{C}_j when the

³We enforce the term ‘‘split’’ over the term ‘‘partition’’ to acknowledge the possibly overlapping regions of the conditional domain.

⁴Here, a vector in which a single element is 1 and all the others are 0.

enabling set of \mathcal{C}_i is also enabled by \mathcal{C}_j , i.e., $\mathcal{T}_{\mathcal{C}_i}^e \subseteq \mathcal{T}_{\mathcal{C}_j}^e$, and
 the configuration region of the second is included in that of the
 first, i.e., $\mathbf{r}_{\mathcal{C}_j} \subset \mathbf{r}_{\mathcal{C}_i}$. However, mostly, this is a byproduct of the
 formulation. In practice, such configurations are easily avoided
 (see Section III-C).

Definition 6 (Configuration Function): At time step k and
 for continuous vector $\mathbf{x}_{c,k}$, the configuration function $\delta_{\mathcal{C}_k}$ of
 the hybrid system H is a Boolean function from $\mathbf{x}_{c,k} \rightarrow \{0, 1\}$
 given by

$$\delta_{\mathcal{C}_k} = \begin{cases} 1, & \text{if } \mathbf{r}_{\mathcal{C}_k} \cap \mathbf{x}_{c,k} \neq \emptyset \\ 0, & \text{otherwise.} \end{cases} \quad (8)$$

When $\delta_{\mathcal{C}_k} = 1$, the configuration region $\mathbf{r}_{\mathcal{C}_k}$ (and by extension,
 the configuration \mathcal{C}_k itself) is said to be *enabled*. Checking $\mathbf{x}_{c,k}$
 against the configuration regions of the grid, hence, allows one
 to determine which transition(s) are enabled at time step k .

Definition 7 (Configuration-Enabling Set): The
 configuration-enabling set $\mathcal{T}_{\mathcal{C}_k}^e$ is the set of transitions τ^j
 whose guards are such that $\phi^j(\mathbf{r}_{\mathcal{C}_k} \cap \mathbf{x}_{c,k}) = 1$. It is empty
 whenever $\delta_{\mathcal{C}_k} = 0$.

Example 2 (Continued): Assume that $\mathbf{x}_{c,k}$ is a box [see
 Fig. 2(c)]. This example has four not subsumed configurations
 $\mathcal{C}_k^{(p)}$, $p = 1, \dots, 4$. They are defined by the following.

- 1) Configuration regions: $\mathbf{r}_{\mathcal{C}_k^{(1)}} = [\underline{\mathbb{X}}_{k,[1,]} \beta_1, \underline{\mathbb{X}}_{k,[2,]} \beta_2]^T =$

$$(\tilde{\mathbf{x}}_{c,k}^0)^T \text{ obtained with } \beta_1 = \beta_2 = \begin{bmatrix} 1 \\ 0 \\ 0 \end{bmatrix}; \mathbf{r}_{\mathcal{C}_k^{(2)}} = (] - \infty, \bar{g}_{1,k}^1,] - \infty, \underline{g}_{2,k}^2,])^T \text{ obtained with } \beta_1 = \begin{bmatrix} 0 \\ 0 \\ 1 \end{bmatrix} \text{ and } \beta_2 = \begin{bmatrix} 0 \\ 1 \\ 0 \end{bmatrix}$$

$$\begin{bmatrix} 1 \\ 0 \\ 0 \end{bmatrix}; \mathbf{r}_{\mathcal{C}_k^{(3)}} = (]\bar{g}_{1,k}^1, +\infty[, \underline{g}_{2,k}^2, +\infty])^T \text{ obtained with } \beta_1 = \begin{bmatrix} 1 \\ 0 \\ 0 \end{bmatrix} \text{ and } \beta_2 = \begin{bmatrix} 0 \\ 1 \\ 1 \end{bmatrix}; \text{ and } \mathbf{r}_{\mathcal{C}_k^{(4)}} = (] - \infty, \bar{g}_{1,k}^1,] - \infty, \underline{g}_{2,k}^2, +\infty])^T \text{ obtained with } \beta_1 = \begin{bmatrix} 0 \\ 1 \\ 0 \end{bmatrix} \text{ and } \beta_2 = \begin{bmatrix} 0 \\ 0 \\ 1 \end{bmatrix}.$$

- 2) Configuration functions $\delta_{\mathcal{C}_k^{(p)}}$, $p = 1, \dots, 4$ with $\delta_{\mathcal{C}_k^{(1)}} =$

$$\delta_{\mathcal{C}_k^{(2)}} = 0 \text{ and } \delta_{\mathcal{C}_k^{(3)}} = \delta_{\mathcal{C}_k^{(4)}} = 1.$$

- 3) Configuration-enabling sets: $\mathcal{T}_{\mathcal{C}_k^{(1)}}^e = \mathcal{T}_{\mathcal{C}_k^{(2)}}^e = \emptyset$; $\mathcal{T}_{\mathcal{C}_k^{(3)}}^e =$

$$\{\tau^2\}; \mathcal{T}_{\mathcal{C}_k^{(4)}}^e = \{\tau^1, \tau^2\}; \text{ the situation is nondeterministic since } \tau^1 \text{ and } \tau^2 \text{ are simultaneously enabled.}$$

C. Condition Variables

Configurations relate subregions of the continuous space to the
 enabling of transitions, which are discrete events. Thus, con-
 figurations are a natural articulation between the continuous and
 discrete dynamics. However, at this stage of the formulation,
 configurations have not yet been directly related to the modes.

The difficulty is that one mode may be consistent with several
 configurations of the hybrid system. Thus, in the thermostat
 example, the *on* mode is consistent with both $x \in] - \infty, x^{\min}]$
 and $x \in]x^{\min}, x^{\max}[$. The opposite is also true since one
 configuration may be consistent with several modes. In the
 same example, modes *on* and *off* are both consistent with

511 $x \in]x^{\min}, x^{\max}[$. In the following, we show how to relate
 512 the configurations to the modes. The final aim is to give a
 513 formal basis for the estimation algorithm to circumvent the
 514 full enumeration of all possible combinations of modes and
 515 configurations. What is sought is thus an articulation of the
 516 configurations with the modes.

517 The solution comes quite naturally. The idea is to reflect the
 518 enabled configurations at the discrete level. The enabled con-
 519 figurations can be expressed within the discrete state through
 520 a set of projection unit vectors: the β_i that define the config-
 521 uration regions (6). However, relation (8) considers only those
 522 regions that intersect $\mathbf{x}_{c,k}$. The solution becomes finding the
 523 subset of vectors β_i that define those configuration regions that
 524 satisfy (8) and including them into the discrete representation of
 525 the state.

526 To differentiate them from other vectors, these unit solution
 527 vectors are noted as $\kappa_d^i = [\kappa_{d0}^i, \kappa_{d1}^i, \dots, \kappa_{dn_T}^i]^T$ for every $i =$
 528 $1, \dots, n_c$. Every κ_{dj}^i has domain $\{0, 1\}$, and we refer to it as
 529 a *conditional variable* since it refers to which portion of the
 530 conditional domain does enable a configuration. κ_d^i is dubbed
 531 as a *conditional vector*.

532 *Definition 8 (Conditional Vectors)*: Given H and its con-
 533 tinuous state $\mathbf{x}_{c,k}$, the conditional vectors $\kappa_d^1, \dots, \kappa_d^{n_c}$ are
 534 unit vectors such that $[\mathbb{X}_{k,[1, \cdot]} \kappa_d^1, \dots, \mathbb{X}_{k,[n_c, \cdot]} \kappa_d^{n_c}]^T \cap \mathbf{x}_{c,k} \neq$
 535 $\emptyset, i = 1, \dots, n_c$.

536 Given $\mathbf{x}_{c,k}$ as a box, there exist many different combinations
 537 of conditional vectors. Every combination extracts an enabled
 538 configuration from \mathbb{X}_k . Finally, we permit additional constraints
 539 among κ_d^i and other discrete variables of X_d to be specified in
 540 Q . This allows discrete variables other than modes to depend
 541 on the continuous state values. Additionally, configurations
 542 that are subsumed can be avoided. These configurations arise
 543 from conditional vectors that extract dimensions that are un-
 544 constrained by the condition functions of some transitions.
 545 Constraining the Boolean values of the associated condition
 546 variables eliminates these solution vectors. See the example
 547 below.

548 *Example 2 (Continued)*: Consider $\mathbb{X}_k = [\tilde{\mathbf{x}}_{c,k}^0, \tilde{\mathbf{x}}_{c,k}^1, \tilde{\mathbf{x}}_{c,k}^2]$
 549 defined earlier. $\tilde{x}_{c1,k}^2 = \tilde{x}_{c2,k}^1 =] - \infty, +\infty[$. Thus, any con-

550 figuration region obtained with solution vectors $\kappa_d^1 = \begin{bmatrix} 0 \\ 0 \\ 1 \end{bmatrix}$

551 and/or $\kappa_d^2 = \begin{bmatrix} 0 \\ 1 \\ 0 \end{bmatrix}$ is subsumed. The constraints to exclude

552 these solution vectors are in Q .

553 *Example 1 (Continued)*: Given $\mathbf{x}_c = x$ and hence $\mathbb{X}_k =$
 554 $[\tilde{x}_k^0, \tilde{x}_k^1, \tilde{x}_k^2, \tilde{x}_k^3, \tilde{x}_k^4]$ defined earlier, the thermostat system uses
 555 one vector $\kappa_d = [\kappa_{d0}, \kappa_{d1}, \kappa_{d2}, \kappa_{d3}, \kappa_{d4}]^T$. Assuming that

556 $]x^{\min}, x^{\max}[\subseteq x_k$, then $\kappa_d = \begin{bmatrix} 1 \\ 0 \\ 0 \\ 0 \\ 0 \end{bmatrix}, \begin{bmatrix} 0 \\ 1 \\ 0 \\ 0 \\ 0 \end{bmatrix}, \begin{bmatrix} 0 \\ 0 \\ 1 \\ 0 \\ 0 \end{bmatrix}, \begin{bmatrix} 0 \\ 0 \\ 0 \\ 1 \\ 0 \end{bmatrix}$, and

557 $\begin{bmatrix} 0 \\ 0 \\ 0 \\ 0 \\ 1 \end{bmatrix}$ are the five conditional solution vectors such that $\mathbb{X}_k \kappa_d \cap$

558 $x_k \neq \emptyset$.

Conditional variables pave the way for the definition of a *log-*
 559 *ical configuration* that articulates the continuous and discrete
 560 states and dynamics. 561

D. Logical Configuration 562

What is referred to as a *logical configuration* is simply the
 563 expression of a configuration at the discrete level. The useful
 564 feature is that logical configurations directly relate to hybrid
 565 system modes. 566

Definition 9 (Logical Configuration): Given a hybrid system
 567 H and its continuous state $\mathbf{x}_{c,k}$ at time step k , a logical
 568 configuration of H is noted as the logical conjunction 569

$$\nabla \delta_k = x_m \wedge \left[\bigwedge_{i=1}^{n_c} \left[\bigwedge_{j=0}^{n_T} (\kappa_{dj}^i = \xi_j) \right] \right]$$

where 570

$$\xi_j = \begin{cases} 1, & \text{if } \kappa_{dj}^i \text{ is the } j\text{th unit vector} \\ 0, & \text{otherwise.} \end{cases}$$

Example 2 (Continued): In Fig. 2(c), the system is in mode
 571 m_1 . We have seen that $\mathcal{C}_k^{(3)}$ and $\mathcal{C}_k^{(4)}$ are enabled. The condi- 572

tional vectors of interest are thus $\kappa_d^1 = \begin{bmatrix} 1 \\ 0 \\ 0 \end{bmatrix}$ and $\kappa_d^2 = \begin{bmatrix} 0 \\ 0 \\ 1 \end{bmatrix}$; 573

$\kappa_d^1 = \begin{bmatrix} 0 \\ 1 \\ 0 \end{bmatrix}$ and $\kappa_d^2 = \begin{bmatrix} 0 \\ 0 \\ 1 \end{bmatrix}$, respectively. This leads to two 574

logical configurations $\nabla \delta_k^{(3)}$ and $\nabla \delta_k^{(4)}$ of the form $\nabla \delta_k^{(p)} =$ 575
 $(x_m = m_1) \wedge [\bigwedge_{i=1}^2 [\bigwedge_{j=0}^2 (\kappa_{dj}^i = \xi_j)]]$. 576

IV. HYBRID STATE ESTIMATION 577

Given a set of commands and observations at every time
 578 step, the set-theoretic estimation of hybrid states consists of
 579 predicting a set of hybrid state candidates and rejecting those
 580 that do not predict the observations. In consequence, most
 581 operations are concerned with prediction. The problem of
 582 prediction is its cost, since many predicted states may end
 583 up being rejected. It is thus essential to eliminate impossible
 584 candidates as early as possible. Prediction consists of a loop at
 585 each sampled time step: continuous prediction, discrete state
 586 prediction, and continuous state transfer, until there are no
 587 more enabled changes in the discrete dynamics. It follows that
 588 early elimination of state candidates is possible at every loop
 589 step. While continuous state elimination simply requires an
 590 inclusion test of the observations, discrete state elimination
 591 requires a full consistency check that is more demanding.
 592 However, this task has connections with a set of techniques
 593 referred to as the consistency-based approach to diagnosis [39].
 594 These techniques use the constraints in the models to limit
 595 the state candidates to be considered [23], [40]. They can
 596 prune out candidates at each step that standard filters would
 597 keep in their set of estimates. In consequence, our algorithms
 598 rely on these techniques to manage discrete state consistency.
 599 To further mitigate the number of candidates, our estimation
 600

601 scheme shows how the modeling of uncertainty in a bounded
 602 form allows us to merge estimates with identical discrete state.
 603 This proves to be a decisive advantage of state estimation
 604 based on uncertain but bounded models over state estimation
 605 based on stochastic models. In addition, our estimator includes
 606 a procedure that estimates several fast successive switches in
 607 discrete dynamics in-between two sampled time steps. Here,
 608 again, a bounded uncertainty is key to allowing this feature.

609 A. Hybrid State Prediction in Sampled Time

610 1) *Forward Time Prediction*: A prediction of the hybrid
 611 state is obtained with a forward predictive operator [41].

612 *Definition 10 (Forward Time Prediction)*: The forward time
 613 prediction $\langle S_{l,k-1} \rangle_\gamma^\wedge$ of a set $S_{l,k-1}$ of hybrid states at logical
 614 time step l and sampled time step $k-1$ is the set of hybrid
 615 states that are reachable from $S_{l,k-1}$ by letting the sampled
 616 time progress over γ sampled steps. For a single hybrid state,
 617 $s_{l,k-1} = (\boldsymbol{\pi}_l, \mathbf{x}_{c,k-1})$, $\boldsymbol{\pi}_l = (x_{m,l}, \mathbf{x}_{d,l})$

$$\langle s_{l,k-1} \rangle_1^\wedge = \{s_{l,k} = (\boldsymbol{\pi}_l, \mathbf{x}_{c,k}) | \mathbf{x}_{c,k} = f(\mathbf{x}_{c,k-1}, \mathbf{u}_{c,k-1}, \mathbf{w}_{c,k-1}, x_{m,l})\} \quad (9)$$

618 and $\langle S_{l,k-1} \rangle_\gamma^\wedge$ is the repetition of $\langle S_{l,k-1} \rangle_1^\wedge$, γ times, over all
 619 $s_{l,k-1} \in S_{l,k-1}$.

620 There are many ways for relation (9) to be efficiently com-
 621 puted. The difficulty is that the box $\mathbf{x}_{c,k}$ keeps growing with the
 622 number of steps γ . This is because the rectangular approxima-
 623 tion at each step introduces an error that is reapproximated by
 624 successive steps and thus rapidly amplified. This phenomenon
 625 is known as the *wrapping effect*. In general, convex optimiza-
 626 tion techniques help mitigate this explosion of uncertainty. In
 627 the current implementation, interval numerical methods similar
 628 to those in [36] are used.

629 While the mechanics of transition triggering are described
 630 later, here, it is enough to mention that two cases arise: 1)
 631 whenever no transition is enabled by the forward time predic-
 632 tion, then the observations $\tilde{\mathbf{y}}_{c,k}$ can be used to prune impossible
 633 candidates; and 2) when a transition is enabled, observations
 634 cannot be used immediately since they may have been produced
 635 by a behavior that is different from that of the current mode and
 636 model. Case 1 corresponds to applying set-theoretic filtering
 637 techniques to forward time prediction. Linear and nonlinear
 638 filters have been described [30]–[33]. In the case of nonlinear
 639 systems, the produced bounded estimates can be approximated
 640 by a variety of geometrical shapes, ellipsoids [33], rectangles
 641 [30], [32], and polytopes [42]. These filters can be utilized to
 642 control the quality of the forward time prediction. In the fol-
 643 lowing, it is assumed that the produced shapes are rectangular
 644 boxes, but the approach can be extended to other shapes as
 645 well.⁵

646 2) *Forward Transition Prediction*: A prediction of the dis-
 647 crete switches is obtained with a second forward predictive
 648 operator.

Definition 11 (Forward Transition Prediction): Given tran- 649
 650 sition τ and a set of hybrid states $S_{l,k}$, the *forward transition*
 651 *prediction* $\langle S_{l,k} \rangle^\tau$ is the set of hybrid states that are reachable
 652 from some state $s_{l,k} \in S_{l,k}$ by executing a transition τ . For
 653 $s_{l,k} = (\boldsymbol{\pi}_l, \mathbf{x}_{c,k})$, with $\boldsymbol{\pi}_l = (x_{m,l}, \mathbf{x}_{d,l})$, if τ is enabled, then 654

$$\langle s_{l,k} \rangle^\tau = \{s_{l+1,k} = (\boldsymbol{\pi}_{l+1}, \mathbf{x}'_{c,k}) | x_{m,l} \xrightarrow{\tau} x_{m,l+1} \text{ and } \mathbf{x}'_{c,k} = l_\tau(\mathbf{x}_{c,k})\} \quad (10)$$

where $\boldsymbol{\pi}_{l+1} = (x_{m,l+1}, \mathbf{x}_{d,l+1})$ such that $Q \cup \boldsymbol{\pi}_{l+1}$ is con- 654
 655 sistent.

By consistent, we mean that $x_{m,l+1}$ and $\mathbf{x}_{d,l+1}$ together 656
 657 satisfy all the formulas in Q .

3) *Hybrid State Prediction*: The hybrid system prediction 658
 659 over time alternates both forward operators. As seen earlier,
 660 multiple transitions can simultaneously be enabled. This is due
 661 to the fact that the box $\mathbf{x}_{c,k}$ can span over several configuration
 662 regions. A consequence is that different points of $\mathbf{x}_{c,k}$ happen to
 663 enable and trigger different transitions, thus leading the system
 664 from its current state to different modes and states. Given a
 665 forward time prediction, the aim of the estimation process is
 666 to transfer each point of the continuous state at date (l, k) to
 667 the possibly multiple mode(s) it belongs to at date $(l+1, k)$.
 668 The solution is to produce a split of $\mathbf{x}_{c,k}$ such that the produced
 669 fragments fit the grid of configurations. The enabled transitions
 670 can then trigger from such state fragments, and the forward
 671 transition prediction yields the new set of modes of the system
 672 along with the set of continuous estimates. 672

B. Hybrid Consistency Problems 673

Given a set of hybrid states $S_{l,k-1}$ at date $(l, k-1)$ and 674
 675 the forward time prediction $S_{l,k} = \langle S_{l,k-1} \rangle_1^\wedge$, the problem of
 676 intersecting $\mathbf{x}_{c,k}$ with the grid of configurations comes to the
 677 finding of a split $P_{l,k} = \{s_{l,k}^{(1)}, \dots, s_{l,k}^{(n_p)}\}$ such that for every
 678 $p = 1, \dots, n_p$, $\mathcal{C}_k^{(p)}$ is a configuration, with $\mathbf{x}_{c,k}^{(p)} \subseteq \mathbf{r}_{c,p}$, and
 679 $\boldsymbol{\pi}_l^{(p)} \cup Q \cup \nabla \delta_k^{(p)}$ is consistent. This is done in two steps.
 680 Given a predicted hybrid state $s_{l,k}$, $\mathbf{x}_{c,k}$ is used to find \mathbb{X}_k
 681 and the conditional vectors $\boldsymbol{\kappa}_d^i$. Those vectors yield the logical
 682 configurations $\nabla \delta_k^{(p)}$ that are consistent with $s_{l,k}$. An initial set
 683 of conditional vectors is easily obtained by iterating the con-
 684 tinuous dimensions and checking whether \mathbb{X}_k intersects $\mathbf{x}_{c,k}$.
 685 Further checking against Q yields the reduced set of logical
 686 configurations that are possible under the set of qualitative con-
 687 straints. Impossible configurations are eliminated. The second
 688 step takes the remaining logical configurations and computes
 689 the configuration regions out of the predicted $\mathbf{x}_{c,k}$. Recall that
 690 every configuration region is shaped by a system of inequalities
 691 over the condition functions g_i^j in (5). These inequalities form a
 692 constraint network among continuous variables. Therefore, the
 693 change of one variable-bounded value often affects the range
 694 of other variables. By iterating a constraint filtering process
 695 over all continuous variables, the focus narrows down onto the
 696 only possible continuous states. The double logical/continuous
 697 formulation of configurations from Section III is key as it
 698 permits the pruning of impossible estimates at both levels. 698

⁵With the limitation that intersection with the grid of configurations may not conserve certain shapes.

699 Basically, the first pruning step takes place at a discrete level,
700 and the second pruning step takes place at the continuous level.
701 Information is passed through the logical configurations.

702 1) *Discrete State Consistency*: Given a hybrid system H
703 and a prediction $s_{l,k} = (\pi_l, \mathbf{x}_{c,k})$, then $\{(\pi_l^{(p)}, \nabla\delta_k^{(p)})\}$, $p =$
704 $1, \dots, n_p$, are such that we have the following:

705 1) They are consistent with Q

$$\pi_l^{(p)} \cup Q \cup \nabla\delta_k^{(p)} \text{ is consistent.} \quad (11)$$

706 2) $\pi_l^{(p)} = (x_{m,l}, \mathbf{x}_{d,l}^{(p)})$, so that the mode estimate $x_{m,l}$ is that
707 of $s_{l,k}$, since no transition has triggered yet.

708 The conditional vectors κ_d^i determine a set of logical con-
709 figurations. A subset of those is selected by solving rela-
710 tion (11). This can be done with a constraint satisfaction
711 engine. Solutions to (11) are logical configurations along
712 with discrete state estimates $\pi_l^{(p)}$. This operation is noted
713 as $\{(\pi_l^{(p)}, \nabla\delta_k^{(p)})\}_{p=1, \dots, n_p} = sat(s_{l,k}, Q)$, where sat denotes
714 the constraint satisfaction engine. In the present implementa-
715 tion, the Boolean satisfaction engine described in [43] is used.
716 A wide range of other techniques is applicable.

717 2) *Continuous State Consistency*: Given a configuration
718 $\mathcal{C}_k^{(p)}$ at the continuous level, the subregion $\mathbf{x}_{c,k}^{(p)}$ of $\mathbf{x}_{c,k}$ that is
719 consistent with the configuration region is given by

$$\mathbf{x}_{c,k}^{(p)} = \mathbf{x}_{c,k} \cap \mathbf{r}_{\mathcal{C}_k^{(p)}}. \quad (12)$$

720 Computing $\mathbf{x}_{c,k}^{(p)}$ is more difficult than it seems. Recall that $\mathbf{r}_{\mathcal{C}_k^{(p)}}$
721 is equal to $[\mathbb{X}_{k,[1, \dots]} \kappa_d^1, \dots, \mathbb{X}_{k,[m_c, \dots]} \kappa_d^{n_c}]^T$, where the κ_d^i 's are
722 given by $\nabla\delta_k^{(p)}$. Every unit vector κ_d^i extracts a positive or
723 negative subdomain from \mathbb{X}_k . Every subdomain is obtained by
724 evaluating a condition function g_j^i , where j is given by the
725 entry equal to 1 of unit vector κ_d^i . To satisfy (12), the points
726 of the box $\mathbf{x}_{c,k}^{(p)}$ must satisfy all the condition functions that
727 determine $\mathbf{r}_{\mathcal{C}_k^{(p)}}$.

728 However, a variable x_{ci} can be coupled with some other
729 variables $x_{ci'}$ through g_j^i . This means that tightening the bounds
730 of x_{ci} has an effect on $x_{ci'}$'s bounds. This problem can be seen
731 as the task of filtering a set of bounded variables x_{ci} with a set
732 of inequalities over those same variables. Such a problem can
733 be solved with a slightly revised version of standard filtering or
734 branch-and-bound techniques. Indeed, in general, these tech-
735 niques do not handle inequalities but only equality constraints
736 [44]. The algorithmic solution in Table II is a variant of the
737 constraint propagation system in [44] that handles inequalities.
738 Prior to detailing the algorithm, admissibility and consistency
739 are to be distinguished.

740 1) A condition function g_j^i is said to be admissible for $\mathbf{x}_{c,k}$
741 iff there exists at least a point of $\mathbf{x}_{c,k}$ such that the
742 inequality based on $g_j^i(\mathbf{x}_{c,k})$ is satisfied.
743 2) $\mathbf{x}_{c,k}$ is said to be consistent with $g_j^i(\mathbf{x}_{c,k})$ when the
744 inequality based on g_j^i is satisfied for all points in $\mathbf{x}_{c,k}$.

745 The algorithm in Table II finds $\mathbf{x}_{c,k}^{(p)}$ such that it is consistent
746 with all of the condition functions g_j^i that determine $\mathbf{r}_{\mathcal{C}_k^{(p)}}$. The
747 algorithm constrains all the variables that appear in the con-

TABLE II
FINDING CONSISTENT CONTINUOUS STATES: $filter(\nabla\delta_k^{(p)}, \mathbf{x}_{c,k})$

Require: $\nabla\delta_k^{(p)}, \mathbf{x}_{c,k}$.
1: Agenda = $\{g_j^i \mid \kappa_d^i \text{ is the } j\text{-th unit vector, } i = 1, \dots, n_c\}$.
2: $\mathbf{x}_{c,k}^{(p)} = \mathbf{x}_{c,k}$.
3: **while** Agenda not empty **do**
4: Select a g_j^i in Agenda.
5: Recompute positive subdomain $\tilde{\mathbf{x}}_{c,k}^j$, i.e. find the $x'_{ci,k} \leq$
 $g_j^i(x_{c1,k}^{(p)}, \dots, x_{ci-1,k}^{(p)}, x_{ci+1,k}^{(p)}, \dots, x_{cn,k}^{(p)})$ such that $\phi_i^j(\mathbf{x}_{c,k}^{(p)}) = 1$.
When $j = 0$, the negative subdomain is recomputed instead.
6: $Int = x'_{ci,k} \cap x_{ci,k}^{(p)}$.
7: **if** $Int = \emptyset$ **then**
8: g_j^i is inadmissible for $\mathbf{x}_{c,k}^{(p)}$.
9: Reject $\nabla\delta_k^{(p)}$.
10: **return** \emptyset .
11: **if** $x_{ci,k}^{(p)} \subseteq x'_{ci,k}$ **then**
12: Remove g_j^i from Agenda.
13: **else**
14: Add $\{g_{i'}^j \mid \kappa_d^{i'} \text{ is the } j\text{-th unit vector, } i' \neq i\}$ to the Agenda.
15: $\mathbf{x}_{c,k}^{(p)} \leftarrow Int$.
16: **return** $\mathbf{x}_{c,k}^{(p)}$.

TABLE III
SPLITTING THE CONTINUOUS SPACE: $split(s_{l,k})$

Require: $s_{l,k}$.
1: $P_{l,k} = \{\}$.
2: Find the combinations of κ_d^i for all $i = 1, \dots, n_c$ that define the $\nabla\delta_k^{(q)}$,
 $q = 1, \dots, n_q$.
3: Compute $\{(\pi_l^{(p)}, \nabla\delta_k^{(p)})\}_{p=1, \dots, n_p} = sat(s_{l,k}, Q)$, $n_p \leq n_q$.
4: **for all** $\nabla\delta_k^{(p)}$ **do**
5: $\mathbf{x}_{c,k}^{(p)} = filter(\nabla\delta_k^{(p)}, \mathbf{x}_{c,k})$.
6: **if** $\mathbf{x}_{c,k}^{(p)} \neq \emptyset$ **then**
7: $s_{l,k}^{(p)} = (\pi_l^{(p)}, \mathbf{x}_{c,k}^{(p)})$.
8: $P_{l,k} \leftarrow P_{l,k} \cup s_{l,k}^{(p)}$.
9: **return** $P_{l,k}$.

dition functions g_j^i drawn from an input logical configuration 748
 $\nabla\delta_k^{(p)}$. It does so until each condition function is either satisfied 749
or inadmissible. The operator described by the algorithm is 750
dubbed $filter(\nabla\delta_k^{(p)}, \mathbf{x}_{c,k})$. Its result is a continuous state 751
fragment $\mathbf{x}_{c,k}^{(p)}$. 752

C. Splitting the Hybrid State With Configurations 753

The operator that articulates sat and $filter$, i.e., the discrete 754
and continuous consistency operators, respectively, is referred 755
to as $split$. $split$ applies to a set $S_{l,k}$ of hybrid states and returns 756
another set $P_{l,k}$ (see Table III). The algorithm takes a predicted 757
hybrid state $s_{l,k}$ as input. 758

Example 2 (Continued): Starting from the configurations 759
obtained in Fig. 2(c), Fig. 3(a) and (b) shows the split of 760
the continuous space for enabled configurations $\mathcal{C}_k^{(3)}$ and $\mathcal{C}_k^{(4)}$, 761
respectively. The logical configurations are $\nabla\delta_k^{(3)}$ and $\nabla\delta_k^{(4)}$ 762
defined earlier. The $filter$ operator applied to each configura- 763
tion reduces $\mathbf{x}_{c,k}$ by using partial guard g_1^1 (step 5, Table II). 764
In both cases, evaluating $g_2^2(\mathbf{x}_{c,k})$ does not further reduce $\mathbf{x}_{c,k}$. 765
The results are then $\mathbf{x}_{c,k}^{(3)}$ and $\mathbf{x}_{c,k}^{(4)}$. 766

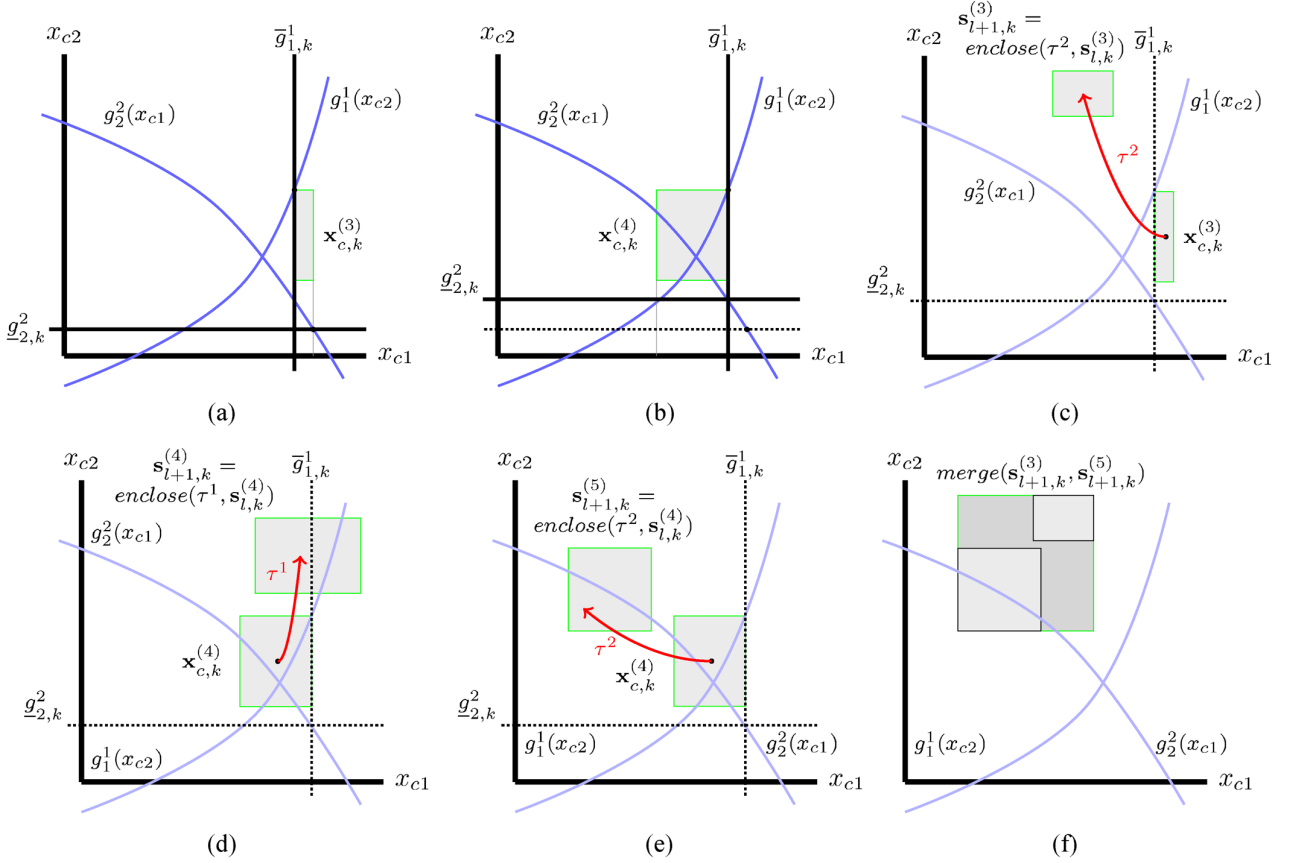


Fig. 3. Example 2. (a) and (b) Continuous state split. On (b), note that the configuration domain has changed: the split with $\bar{g}_{1,k}^1$ affects the value of $\underline{g}_{2,k}^2$. The dotted line shows the previous boundary. (c), (d), and (e) Enclosure and switches according to $\mathcal{T}_{C_k^{(3)}}^e = \{\tau^2\}$ and $\mathcal{T}_{C_k^{(4)}}^e = \{\tau^1, \tau^2\}$. Only the late switch is represented. $\mathbf{s}_{l+1,k}^{(3)} = \text{enclose}(\tau^2, \mathbf{s}_{l,k}^{(3)})$, $\mathbf{s}_{l+1,k}^{(4)} = \text{enclose}(\tau^1, \mathbf{s}_{l,k}^{(4)})$, and $\mathbf{s}_{l+1,k}^{(5)} = \text{enclose}(\tau^2, \mathbf{s}_{l,k}^{(4)})$. (f) Merging step. The estimates obtained in (c) and (e) have identical mode m_3 . In consequence, their continuous estimates can be merged. (a) Split with configuration $C_k^{(3)}$. (b) Split with configuration $C_k^{(4)}$. (c) Triggering of τ^2 from $C_k^{(3)}$. (d) Triggering of τ^1 from $C_k^{(4)}$. (e) Triggering of τ^2 from $C_k^{(4)}$. (f) Merging of (c) and (e).

767 In all cases, remark that the union of the continuous state
768 fragments yields the originally predicted state. That is, the $\mathbf{x}_{c,k}^{(p)}$,
769 $p = 1, \dots, n_p$, that result from the split of a state $\mathbf{x}_{c,k}$ are such
770 that $\bigcup_{p=1}^{n_p} \mathbf{x}_{c,k}^{(p)} = \mathbf{x}_{c,k}$. Formally, this is because the conditional
771 domain \mathbb{X}_k of $\mathbf{x}_{c,k}$ contains the positive and negative subdo-
772 mains $\tilde{\mathbf{x}}_{c,k}^j$ and $-\tilde{\mathbf{x}}_{c,k}^j$ for all transitions τ^j . Therefore, the entire
773 continuous state space is covered by configuration regions, and
774 both $\mathbf{x}_{c,k} \subseteq \bigcup_{p=1}^{n_p} \mathbf{r}_{C_k^{(p)}}$ and $\bigcup_{p=1}^{n_p} \mathbf{x}_{c,k}^{(p)} = \bigcup_{p=1}^{n_p} (\mathbf{r}_{C_k^{(p)}}) \cap \mathbf{x}_{c,k}$
775 [from relation (12)] hold.

776 However, the hybrid states produced by a split are rarely
777 optimal: some hybrid states are, in fact, not reachable by the
778 system. This is due to a lack of constraints between modes
779 and conditional variables in logical configuration equations. In
780 example 1, hybrid state $s_k = (x_m = \text{on} \wedge x_k)$ with $x_k \geq x_k^{\max}$
781 is unreachable but predicted at some point: the thermostat
782 cannot be turned on, and the temperature can be over the upper
783 threshold x_k^{\max} . The problem is complex, as these configura-
784 tions represent the so-called *mythical states* [28], [45]–[47], i.e.,
785 *instantaneous* states between normal states when a discontinu-
786 ous change takes place. In a mythical state, the variables do
787 not satisfy all of the system constraints. This happens to be

the case of the state s_k above, since a transition to the mode 788
789 *off* is enabled but has not triggered yet. The problem is that 789
790 it is not clear whether these states represent very short but real 790
791 instances, or whether they are artifacts of the representation and 791
792 reasoning procedures. For this reason, the *split* operator is said 792
793 to be complete but unsound. 793

D. Switching in Sampled Time

794

When the split is completed, some of the configuration-795
796 enabling sets are not empty. The two final steps of the 796
797 estimation process are thus the triggering of the enabled tran-797
798 sitions and the use of available observations. The triggering 798
799 of transitions at a sampled time raises the following two 799
800 problems. 800

- 1) A transition triggering is always considered a small 801
802 period of time after the real switch has occurred. A 802
803 consequence is that $\mathbf{x}_{c,k}$ computed at time step k is not 803
804 guaranteed to capture the real behavior of the system. 804
- 2) Multiple successive switches may occur during a single 805
806 sampled time interval. 806

TABLE IV

 APPLIES TRANSITION τ ENABLED AT TIME STEP $(l, k) : \text{enclose}(\tau, \mathbf{s}_{l,k}^{(p)})$

Require: $\mathbf{s}_{l,k}^{(p)} = (\boldsymbol{\pi}_l^{(p)}, \mathbf{x}_{c,k}^{(p)})$, enabled transition τ .

- 1: Late switch: $\mathbf{s}'_{l+1,k} = (\boldsymbol{\pi}'_{l+1}, \mathbf{x}'_{c,k}) = \langle \mathbf{s}_{l,k}^{(p)} \rangle^\tau$.
- 2: Early switch: $\mathbf{s}^*_{l+1,k-1} = (\boldsymbol{\pi}^*_{l+1}, \mathbf{x}^*_{c,k-1})$ with $\mathbf{x}^*_{c,k-1} = l_\tau(\bar{\mathbf{x}}_{c,k-1})$
and $\bar{\mathbf{x}}_{c,k-1} = \mathbf{x}_{c,k-1} \cup \bar{\mathbf{r}}_{C_{k-1}^{(p)}}$.
- 3: Prediction after the early switch: $\mathbf{s}^*_{l+1,k} = \langle \mathbf{s}^*_{l+1,k-1} \rangle_1^\tau$.
- 4: update: $\mathbf{x}_{c,k}^{(p)} = [\min(\mathbf{x}^*_{c,k}, \mathbf{x}'_{c,k}), \max(\mathbf{x}^*_{c,k}, \mathbf{x}'_{c,k})]$.
- 5: **return** $\mathbf{s}_{l+1,k}^{(p)} = (\boldsymbol{\pi}_{l+1}^{(p)}, \mathbf{x}_{c,k}^{(p)})$.

TABLE V

 $\text{switch}(S_{l,k})$ OPERATOR

Require: $S_{l,k}, \xi = 0$.

- 1: **while** $\exists \tau$ enabled in $S_{l,k}$ **do**
- 2: $\mathbf{s}_{l+\xi+1,k} = \text{enclose}(\tau, \mathbf{s}_{l+\xi,k})$,
- 3: $\xi \leftarrow \xi + 1$.
- 4: $S_{l+\xi,k} = \text{split}(\mathbf{s}_{l+\xi,k})$.
- 5: $S_{l+\xi,k} = \text{split}(S_{l+\xi,k})$.
- 6: $\text{clear}(S_{l+\xi,k}, \tilde{\mathbf{y}}_{d,k}, \tilde{\mathbf{y}}_{c,k})$.
- 7: $\text{merge}(S_{l+\xi,k})$.
- 8: **return** pruned $S_{l+\xi,k}$.

TABLE VI

 $\text{clear}(S_{l,k})$ OPERATOR

Require: $S_{l,k}, \tilde{\mathbf{y}}_{c,k}, \tilde{\mathbf{y}}_{d,k}$.

- 1: **for all** $\mathbf{s}_{l,k} \in S_{l,k}$ **do**
- 2: **if** $\tilde{\mathbf{y}}_{c,k} \not\subseteq \mathbf{y}_{c,k}$ or $\tilde{\mathbf{y}}_{d,k} \wedge \mathbf{x}_{d,k}$ is inconsistent **then**
- 3: Remove $\mathbf{s}_{l,k}$ from $S_{l,k}$.
- 4: **return** $S_{l,k}$.

807 1) *Guaranteed Enclosure at Switching Points:* The problem
 808 arises from the triggering of a transition in-between two sam-
 809 pled time steps. At time step $k - 1$, no transition is enabled.
 810 Prediction produces a set of hybrid states at time step k . The
 811 *split* operator applies and splits the continuous state according
 812 to candidate configurations. As a result, assume that some
 813 configurations are found to enable transitions at time step k ,
 814 and consider an enabled transition τ . On the physical system,
 815 τ has triggered somewhere between sampled time steps $k - 1$
 816 and k . However, prediction proceeds by computing a late switch
 817 at time step k . Let $\mathbf{x}_{c,k'}$, $k - 1 < k' \leq k$, be the continuous
 818 state at the unknown continuous time instant $k'T_s$ at which
 819 the transition has triggered on the physical system and where
 820 $k' \in \mathfrak{R}$. In general, $\mathbf{x}_{c,k'} \not\subseteq \mathbf{x}_{c,k}$, so switching at k misses the
 821 transfer of some continuous regions.

822 A solution is proposed to transfer the continuous state from
 823 one mode to another, which guarantees to capture the true
 824 behavior of the system. It computes an early switch at $k - 1$,
 825 in addition to the late switch at k . Under the assumption
 826 that the continuous evolution of the system is monotonous
 827 between two sampled time steps, unionizing the continuous
 828 vectors obtained from both switches yields an enclosure of
 829 the true physical state of the system. In practice, due to high
 830 sampling rates, the assumption above is realistic and found
 831 in another body of works [36]. Table IV details the operator
 832 $\text{enclose}(\tau, \mathbf{s}_{l,k}^{(p)})$ that applies a transition τ to a state fragment

833 $\mathbf{s}_{l,k}^{(p)}$ and transfers the continuous state from $\mathbf{s}_{l,k}^{(p)}$ to $\mathbf{s}_{l+1,k}^{(p)}$. The
 834 algorithm returns $\mathbf{s}_{l+1,k}^{(p)}$ that is guaranteed to capture the true
 835 state of the system under the assumption above. The sole subtle
 836 operation of the algorithm is step 2, which *virtually* enables a
 837 switch at time step $k - 1$. This is required since τ cannot be
 838 enabled at time step $k - 1$, as if it were, it would have triggered
 839 at that time step. Therefore, τ has to be virtually enabled at
 840 $k - 1$. This is achieved by triggering τ from the union of $\mathbf{x}_{c,k-1}^{(p)}$
 841 and the frontier $\bar{\mathbf{r}}_{C_{k-1}^{(p)}}$ of the configuration region that enables τ .

842 Note that the algorithm requires working on a temporal window
 843 of at least two sampled time steps, and that both $\mathbf{r}_{C_{k-1}^{(p)}}$ and
 844 $\mathbf{x}_{c,k-1}^{(p)}$ must remain accessible in memory.

845 *Example 2 (Continued):* Fig. 3(c)–(e) shows the triggering
 846 of the enabled transitions τ^1 and τ^2 . On these figures, only the
 847 late switch is represented. We have $\mathbf{s}_{l+1,k}^{(3)} = \text{enclose}(\tau^2, \mathbf{s}_{l,k}^{(3)})$,
 848 $\mathbf{s}_{l+1,k}^{(4)} = \text{enclose}(\tau^1, \mathbf{s}_{l,k}^{(4)})$, and $\mathbf{s}_{l+1,k}^{(5)} = \text{enclose}(\tau^2, \mathbf{s}_{l,k}^{(4)})$.

2) *Multiple Successive Switches:* When more than one 849
 switch occurs between two sampled time steps, each switch 850
 is successively predicted with the *enclose* operator. Operator 851
switch in Table V handles multiple switches in-between two 852
 sampled time steps. The number of successive switches is noted 853
 as ξ . At step 6, *clear* is the operator that prunes out the states 854
 that do not intersect the observations (Table VI). At step 7, 855 **AOI**
 the operator *merge* optimizes the final partition by merging 856
 hybrid states whenever this is possible. These two operators are 857
 detailed in the two next paragraphs. A condition for *switch* 858
 to terminate is that the hybrid system's behavior *excludes* 859
infinitely many switches occurring in-between two sampled 860
time steps. Whenever this condition is fulfilled, the algorithm 861
 in theory always terminates. In practice, however, the *enclose* 862
 operator yields conservative bounds and adds up to the natural 863
 nonconvergence of numerical uncertainty. In consequence, the 864
 occurrence of infinitely many switches cannot be ruled out, but 865
 a theoretical analysis is beyond the scope of this paper. 866

3) *Recursive Estimation:* Finally, the estimation of the 867
 states of a hybrid system H is captured by a sequence $\rho : 868$
 $S_0, \dots, S_{l,k}, \dots$ that verifies 869

$$S_0 = \text{switch}(\text{split}(\langle \Theta \rangle_0^\zeta)) \quad (13)$$

$$S_{l+\xi,k+\gamma} = \text{switch}(\text{split}(\langle S_{l,k} \rangle_\gamma^\zeta)). \quad (14)$$

Relation (13) initializes the hybrid states starting from the 870
 system initial conditions Θ . The computation of the recursive 871
 relation (14) alternates forward time and transition predictions 872
 through *splits* and *switches*, and results in an updated set of 873
 hybrid states every $\gamma \neq 0$ sampled time steps. 874

E. Hybrid State Estimation

875

The *clear* operator prunes out all the state estimates $\mathbf{s}_{l,k}$ 876
 such that the prediction $\mathbf{y}_{c,k}$ does not enclose the observations 877
 $\tilde{\mathbf{y}}_{c,k}$, or that do not predict observations $\tilde{\mathbf{y}}_{d,k}$. Note that the 878
 measurement noise is already taken into account in (3), so that 879
 $\tilde{\mathbf{y}}_{c,k}$ is a real-valued vector of \mathfrak{R}^{n_y} . 880

TABLE VII
Merge($S_{l,k}$) OPERATOR

| Require: $S_{l,k}$. | |
|----------------------|--|
| 1: | Group the $s_{l,k} \in S_{l,k}$ into $\{S_{l,k}^{(1)}, \dots, S_{l,k}^{(n_q)}\}$ such that all $s_{l,k}^{(i,j)} \in S_{l,k}^{(i)}$ have the same discrete state estimate $\pi_l^{(i)}$. |
| 2: | for $i = 1, \dots, q$ do |
| 3: | $s_{l,k}^{i,1} = (\pi_l^i, \bigcup_{j=1}^{n_q} \mathbf{x}_{c,k}^{(i,j)})$. |
| 4: | For all $j > 1$, remove all $s_{l,k}^{(i,j)}$ from $S_{l,k}$. |
| 5: | return $S_{l,k}$. |

881 F. Merging Identical Discrete Estimates

882 Most approaches to the estimation of hybrid states apply
883 Bayesian belief updates to a stochastic hybrid system. These
884 techniques have to deal with an exponential blowup in the
885 number of possible hybrid states. We can witness a similar
886 effect in our case since the *switch* operator generates a growing
887 number of states at each time step. Adding up to the growing
888 uncertainty that is due to the box approximation of the forward
889 prediction operator, the growth rate of new state estimates
890 rapidly increases. In general, this is the reason why modern es-
891 timators simultaneously track several hybrid state hypotheses.
892 However, inevitably, the number of states exponentially grows
893 with time as more hypotheses become likely.

894 The main advantage of our approach is that it permits the
895 merging of similar trajectories without loss. Consider merging
896 the uncertainty on two states $s_{l,k}^{(1)}$ and $s_{l,k}^{(2)}$: the question is how
897 to merge the two continuous vector estimates $\mathbf{x}_{c,k}^{(1)}$ and $\mathbf{x}_{c,k}^{(2)}$. It
898 is easily achieved by unionizing the variable estimated bounds.
899 The sole condition for the merging is that the discrete states
900 $\pi_{l,k}^{(1)}$ and $\pi_{l,k}^{(2)}$ are identical. The *Merge* operator is given by
901 Table VII. When splits and switches augment the number of
902 hybrid state estimates at each time step, the merging step does
903 reduce this number substantially. In general, this allows the
904 estimation procedure to mitigate the explosion of modes and to
905 maintain a finite, almost constant, number of hybrid estimates.

906 *Example 2 (Continued)*: There are three estimates, which are
907 represented in Fig. 3(c)–(e). In Fig. 3(c), τ^2 has transferred
908 the system state to $s_{l+1,k}^{(3)} = (m_3, \mathbf{x}_{c,k}^{(3)})$. In Fig. 3(d), τ^1 has
909 transferred the system state to $s_{l+1,k}^{(4)} = (m_2, \mathbf{x}_{c,k}^{(4)})$. In Fig. 3(e),
910 τ^2 has transferred the system state to $s_{l+1,k}^{(5)} = (m_3, \mathbf{x}_{c,k}^{(5)})$.
911 $s_{l+1,k}^{(3)}$ and $s_{l+1,k}^{(5)}$ can then be merged. This is shown in Fig. 3(f).
912 Merging the uncertainty is particularly efficient to counter the
913 effects of the occurrence of multiple similar splits and switches,
914 which are a consequence of the temporal uncertainty due to
915 variable bounds. In general, the uncertainty on the continuous
916 state translates into the occurrence of the same transition switch
917 over several time steps. Such situations are common and lead to
918 the production of many estimates with an identical discrete state
919 within just a few time steps. Using a merge operator, it takes
920 just a few more time steps to produce a single estimate instead.
921 However, the actual implementation behind the \bigcup operation on
922 line 3 of Table VII yields a conservative outer approximation
923 of the merged estimates in the shape of a hypercube. This
924 operation introduces an error, because, in general, the union
925 of hypercubes does not yield a hypercube. In our example, the
926 error is visible in Fig. 3(f).

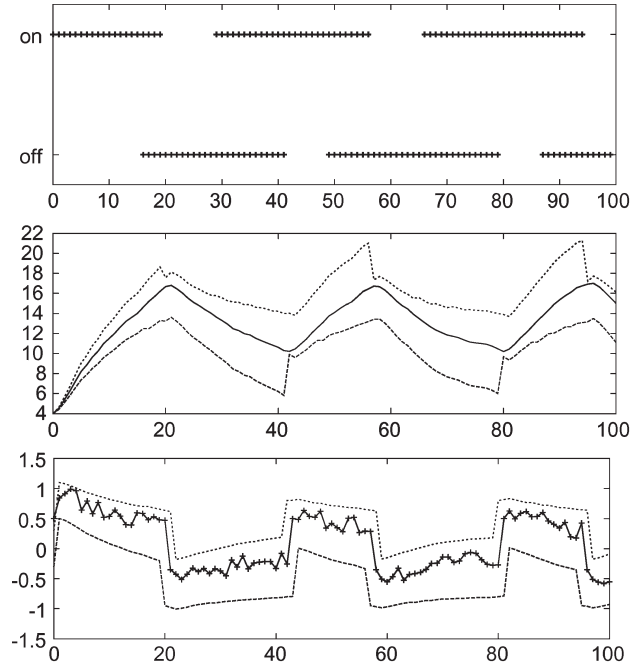


Fig. 4. Set-theoretic estimation of the hybrid state of a thermostat system (Example 1). (Top figure) Mode estimation. (Middle figure) Temperature (in Celsius). (Bottom figure) Temperature variation. All figures: X-axis is time.

Thus, in practice, the merging process enlarges the estimated
927 bounds and reduces the number of estimates. However, the
928 bounds remain guaranteed to enclose the true behavior of the
929 system. However, the additional error carried by the bounds
930 does affect the soundness of the estimator, which produces esti-
931 mates that would not be reachable otherwise. A consequence is
932 that in practice, our hybrid estimation process is complete but
933 unsound. 934

V. RESULTS 935

A preliminary version of the presented filter was imple-
936 mented in C++ as part of a hybrid system diagnosis platform. 937

A. Case Studies 938

Fig. 4 shows the result of a run on our thermostat example. In
939 addition to the thermostat example, the state estimation scheme
940 presented in this paper has been applied to the bi-tanks water
941 regulation system in [48]. This system maintains an outflow of
942 water to a virtual consumer. It models two water tanks, three
943 valves, and a pump. As such, the model totals 1350 possible
944 modes, each of which represents a combination of functional
945 modes for all components in the system. Results on running
946 our estimator on these two systems follow. 947

B. General Performances 948

We have studied the computation time of the estimate as well
949 as the number of state estimates maintained by our filter. The
950 results are reported in Figs. 5 and 6. Fig. 5 illustrates the double
951 advantage of state estimation based on models with bounded
952 uncertainty over Bayesian filtering. First, the highest number of
953

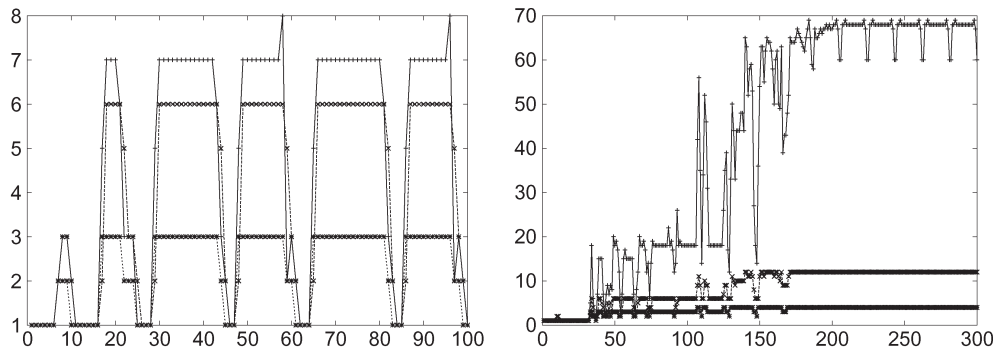


Fig. 5. Number of estimates before and after the merging step. (Left) Thermostat. (Right) Bi-tanks. (Top curve) Hybrid estimates before merging. (Middle curve) Continuous estimates before merging. (Lower curve) Hybrid estimates after merging.

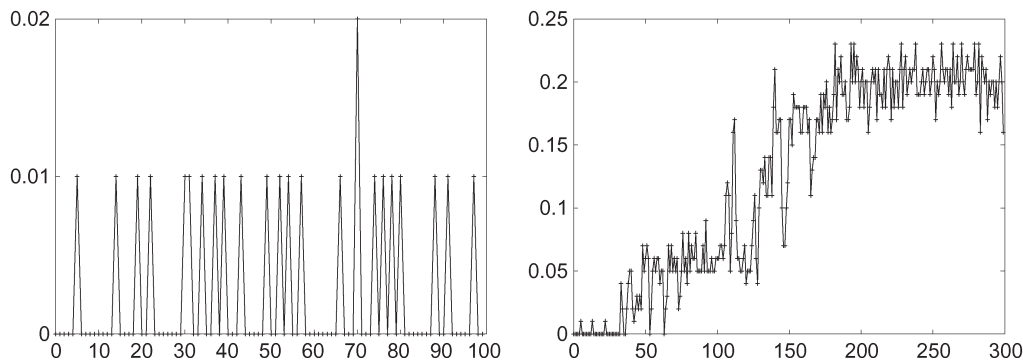


Fig. 6. Computation time per sampled time step (in seconds). (Left) Thermostat. (Right) Bi-tanks.

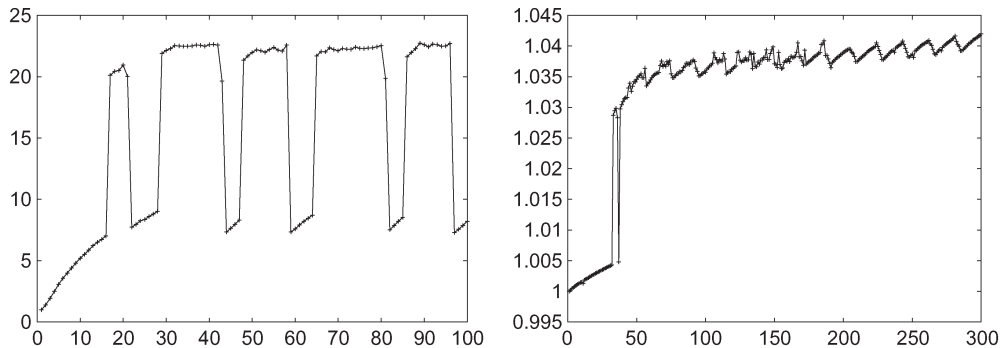


Fig. 7. Relative growth of the bounded uncertainty $\|\mathbf{x}_{c,k}\|/\|\mathbf{x}_{c,0}\|$ over time. (Left) Thermostat. (Right) Bi-tanks.

954 estimated hybrid states is before the merging step and remains
 955 low. For the bi-tanks, this number is around 70, that is, at
 956 worst 5% of all the possible states. Second, the merging step
 957 drastically reduces the total number of hybrid estimates down
 958 to five estimates in the worst case for the bi-tanks. It appears that
 959 the computation time is best correlated with the number of state
 960 estimates before the merging step is applied (see Fig. 6). Note
 961 that comparison with stochastic filters is not directly feasible.

962 C. Uncertainty

963 The discrete switches in a system's dynamics have an effect
 964 on the number of state estimates. Based on the same runs as

before, we aimed to elucidate the effect of bounded uncertainty
 965 on state estimation. Since bounds do not converge, uncertainty
 966 is expected to grow unconditionally with time. Fig. 7 reports
 967 that the uncertainty is growing steadily, but is mitigated by
 968 the switches in the continuous dynamics. This property is
 969 explained by the switching mechanism presented in this paper.
 970 Each switch can help decrease uncertainty in the continuous
 971 state vector: by splitting the continuous state, a switch dis-
 972 cards a subregion of the continuous state space. However,
 973 the uncertainty grows again invariably until the next switch
 974 occurs. 975

This behavior again contrasts with the stochastic hybrid
 976 filters that can shift and focus a probability distribution around
 977

978 subregions of the continuous state space but cannot scale their
979 number of estimates accordingly.

980

VI. CONCLUSION

981 This paper has presented a set-theoretic alternative to the
982 estimation of hybrid systems. It has highlighted the benefits
983 of the approach compared to the dominant estimation scheme
984 that utilizes continuous probability distributions to represent
985 uncertainty. At the core of this paper are the configurations and
986 logical configurations that articulate the discrete and continuous
987 knowledge levels and permit dedicated algorithms to prune
988 impossible estimates at each level. Because bounds do not
989 converge, and due to a conservative merging of estimates, the
990 outer approximation of the continuous state is expected to
991 grow unconditionally with time. Potential solutions include the
992 application of aggressive optimization techniques that produce
993 tighter bounds, and the use of more expressive geometrical
994 shapes. In application to large systems, the computational
995 burden of the next state expansion can prove prohibitive. As
996 a solution, transition selection through sampling or forward
997 search can be implemented as for stochastic hybrid filters at
998 the cost of losing completeness. More research should concen-
999 trate on bridging stochastic model-based estimators and their
1000 set-theoretic counterpart. In general, a pdf badly mixes with
1001 bounded spaces. Thus, the uniform distribution proves unpro-
1002 ductive, because it is not closed under standard operations.
1003 However, some pieces of work have been produced [49], and
1004 a comparison of stochastic and set-theoretic estimation proce-
1005 dures for continuous systems can be found in [50]. This issue is
1006 undoubtedly a promising research direction for the future.

1007

ACKNOWLEDGMENT

1008 The authors would like to thank the anonymous reviewers
1009 for their valuable help in improving this paper.

1010

REFERENCES

- 1011 [1] X. Li and Y. Bar-Shalom, "Multiple-model estimation with variable
1012 structure," *IEEE Trans. Autom. Control*, vol. 41, no. 4, pp. 478–493,
1013 Apr. 1996.
- 1014 [2] P. Hanlon and P. Maybeck, "Multiple-model adaptive estimation using a
1015 residual correlation Kalman filter bank," *IEEE Trans. Aerosp. Electron.
1016 Syst.*, vol. 36, no. 2, pp. 393–406, Apr. 2000.
- 1017 [3] I. Hwang, H. Balakrishnan, and C. J. Tomlin, "State estimation for
1018 hybrid systems: Applications to aircraft tracking," *Proc. Inst. Elect.
1019 Eng.—Control Theory Appl.*, vol. 153, no. 5, pp. 556–566, Sep. 2006.
- 1020 [4] S. McIlraith, G. Biswas, D. Clancy, and V. Gupta, "Towards diagnosing
1021 hybrid systems," in *Proc. 10th Int. Workshop Principles Diagnosis DX-99*,
1022 1999.
- 1023 [5] S. Narasimhan and G. Biswas, "Efficient diagnosis of hybrid systems
1024 using models of the supervisory controller," in *Proc. 12th Int. Workshop
1025 Principles Diagnosis DX-01*, Italy, 2001. Sansicario, Via Lattea.
- 1026 [6] S. Narasimhan, R. Dearden, and E. Benazera, "Combining particle filter
1027 and consistency-based approaches for monitoring and diagnosis of sto-
1028 chastic hybrid systems," in *Proc. 15th Int. Workshop Principles Diagnosis
1029 DX-04*, 2004.
- 1030 [7] S. Narasimhan and L. Brownston, "Hyde—A general framework for sto-
1031 chastic and hybrid model-based diagnosis," in *Proc. 18th Int. Workshop
1032 Principles Diagnosis DX-07*, 2007, pp. 162–169.
- 1033 [8] S. Narasimhan and G. Biswas, "Model-based diagnosis of hybrid sys-
1034 tems," *IEEE Trans. Syst., Man, Cybern. A, Syst., Humans*, vol. 37, no. 3,
1035 pp. 348–361, May 2007.
- [9] A. Doucet, N. de Freitas, K. Murphy, and S. Russel, "Rao-blackwellized
particle filtering for dynamic Bayesian networks," in *Proc. 18th Int. Conf.
Uncertainty Artif. Intell.*, 2002, pp. 176–183.
- [10] F. Hutter and R. Dearden, "The Gaussian particle filter for diagnosis of
non-linear systems," in *Proc. 13th Int. Workshop Principles Diagnosis
DX-03*, 2003, pp. 65–70.
- [11] S. Funiak and B. Williams, "Multi-modal particle filtering for hybrid
systems with autonomous mode transitions," in *Proc. 13th Int. Workshop
Principles Diagnosis DX-03*, 2003.
- [12] U. Lerner, R. Parr, D. Koller, and G. Biswas, "Bayesian fault de-
tection and diagnosis in dynamic systems," in *Proc. AAAI/IAAI*, 2000,
pp. 531–537.
- [13] U. Lerner, B. Moses, M. Scott, S. McIlraith, and D. Koller, "Moni-
toring a complex physical system using a hybrid dynamic Bayes net,"
in *Proc. UAI*, 2002, pp. 301–310.
- [14] M. Hofbaur and B. Williams, "Hybrid estimation of complex
systems," *IEEE Trans. Syst., Man, Cybern. B, Cybern.*, vol. 34, no. 5,
pp. 2178–2191, Oct. 2004.
- [15] N. de Freitas, R. Dearden, F. Hutter, R. Morales-Menendez, J. Mutch,
and D. Poole, "Diagnosis by a waiter and a Mars explorer," *Proc.
IEEE—Special Issue on Sequential State Estimation*, vol. 92, no. 3,
pp. 455–468, Mar. 2004.
- [16] O. Martin, "Diagnosis as approximate belief state enumeration for
probabilistic concurrent constraint automata," in *Proc. 20th Nat. Conf.
Artif. Intell.*, 2005.
- [17] H. Blom and Y. Bar-Shalom, "The interacting multiple model algo-
rithm for systems with Markovian switching coefficients," *IEEE Trans.
Autom. Control*, vol. 33, no. 8, pp. 780–783, Aug. 1998.
- [18] L. Johnston and V. Krishnamurthy, "An improvement to the interacting
multiple model (IMM) algorithm," *IEEE Trans. Autom. Control*, vol. 49,
no. 12, pp. 2909–2923, Dec. 2001.
- [19] V. Verma, S. Thrun, and R. Simmons, "Variable resolution particle filter,"
in *Proc. 18th Int. Joint Conf. Artif. Intell.*, 2003, pp. 976–984.
- [20] S. Thrun, J. Langford, and V. Verma, "Risk sensitive particle filters," in
Proc. NIPS, 2001, pp. 961–968.
- [21] C. Plagemann, D. Fox, and W. Burgard, "Efficient failure detection on
mobile robots using particle filters with Gaussian process proposals," in
Proc. 20th Int. Joint Conf. Artif. Intell., 2007, pp. 2185–2190.
- [22] L. Blackmore, S. Funiak, and B. Williams, "Combining stochastic and
greedy search in hybrid estimation," in *Proc. 20th Nat. Conf. Artif. Intell.*,
2005, pp. 282–287.
- [23] P. Nayak and J. Kurien, "Back to the future for consistency-based trajec-
tory tracking," in *Proc. AAAI*, Austin, TX, 2000, pp. 370–377.
- [24] E. Benazera and S. Narasimhan, "An extension to the Kalman filter for an
improved detection of unknown behavior," in *Proc. 24th Amer. Control
Conf.*, Jun. 2005, pp. 1039–1041.
- [25] F. Cozman and E. Krotkov, "Truncated Gaussians as tolerance sets,"
Robot. Inst., Carnegie Mellon Univ., Pittsburgh, PA, Tech. Rep. CMU-
RI-TR-94-35, Sep. 1994.
- [26] M. Hofbaur and B. Williams, "Mode estimation of probabilistic hybrid
systems," in *Proc. HSCC*, 2002, vol. 2289, pp. 253–266.
- [27] D. S. Weld and J. D. Kleer, *Readings in Qualitative Reasoning About
Physical Systems*. San Mateo, CA: Morgan Kaufmann, 1990.
- [28] B. J. Kuipers, *Qualitative Reasoning: Modeling and Simulation With
Incomplete Knowledge*. Cambridge, MA: MIT Press, 1994.
- [29] P. Combettes, "The foundations of set theoretic estimation," *Proc. IEEE*,
vol. 81, no. 2, pp. 182–208, Feb. 1993.
- [30] M. Milanese and A. Vicino, "Estimation theory for nonlinear models and
set membership uncertainty," *Automatica*, vol. 47, no. 2, pp. 403–408,
Mar. 1991.
- [31] A. Vicino and G. Zappa, "Sequential approximation of feasible parameter
sets for identification with set membership uncertainty," *IEEE Trans.
Autom. Control*, vol. 41, no. 6, pp. 774–785, Jun. 1996.
- [32] L. Jaulin, "Interval constraint propagation with application to bounded-
error estimation," *Automatica*, vol. 36, no. 10, pp. 1547–1552, 2000.
- [33] U. Hanebeck, "Recursive nonlinear set-theoretic estimation based on
pseudo ellipsoids," in *Proc. IEEE Conf. Multisensor Integr. Intell. Syst.*,
2001, pp. 159–164.
- [34] C. Combastel, "A state bounding observer for uncertain non-linear
continuous-time systems based on zonotopes," in *Proc. IEEE CDC*,
Seville, Spain, Dec. 2005, pp. 7228–7234.
- [35] J. Armengol, J. Vehi, L. Travé-Massuyès, and M. Sainz, "Interval model-
based fault detection using multiple sliding time windows," in *Proc. 4th
SAFEPROCESS*, Budapest, Hungary, 2000, pp. 168–173.
- [36] T. A. Henzinger, B. Horowitz, R. Majumdar, and H. Wong-Toi, "Beyond
HYTECH: Hybrid systems analysis using interval numerical methods," in
Proc. HSCC, 2000, pp. 130–144.

- 1113 [37] E. Benazera and L. Travé-Massuyès, "The consistency approach to the
1114 on-line prediction of hybrid system configurations," in *Proc. IFAC Conf.*
AQ6 1115 *Anal. Des. Hybrid Syst.*, 2003.
- 1116 [38] M. Branicky, V. Borkar, and S. Mitter, "A unified framework for hybrid
1117 control: Model and optimal control theory," *IEEE Trans. Autom. Control*,
1118 vol. 43, no. 1, pp. 31–45, Jan. 1998.
- 1119 [39] W. Hamscher, L. Console, and J. D. Kleer, *Readings in Model-Based*
1120 *Diagnosis*. San Mateo, CA: Morgan Kaufmann, 1992.
- 1121 [40] B. C. Williams and P. Nayak, "A model-based approach to reactive
1122 self-configuring systems," in *Proc. AAAI*, Portland, OR, 1996,
1123 pp. 971–978.
- 1124 [41] R. Alur, C. Courcoubetis, N. Halbwachs, T. Henzinger, P.-H. Ho,
1125 X. Nicollin, A. Olivero, J. Sifakis, and S. Yovine, "The algorithmic analysis
1126 of hybrid systems," in *Proc. 11th Int. Conf. Anal. Optim. Discrete*
1127 *Event Syst.*, 1995, pp. 331–351.
- 1128 [42] J. Shamma and K. Tu, "Approximate set-valued observers for nonlinear
1129 systems," *IEEE Trans. Autom. Control*, vol. 42, no. 5, pp. 648–658,
1130 May 1997.
- 1131 [43] B. C. Williams and P. Nayak, "Fast context switching in real-time reason-
1132 ing," in *Proc. AAAI*, Providence, RI, 1997, pp. 50–56.
- 1133 [44] E. Hyvonen, "Constraint reasoning based on interval arithmetic: The tol-
1134 erance propagation approach," *Artif. Intell.*, vol. 58, no. 1–3, pp. 71–112,
1135 Dec. 1992.
- 1136 [45] J. D. Kleer and J. S. Brown, "A qualitative physics based on confluences,"
1137 *Artif. Intell.*, vol. 24, no. 1–3, pp. 7–83, Dec. 1984.
- 1138 [46] T. Nishida and S. Doshita, "Reasoning about discontinuous change," in
1139 *Proc. AAAI*, 1987, pp. 643–648.
- 1140 [47] Y. Iwasaki, A. Farquhar, V. Saraswat, D. Bobrow, and V. Gupta, "Model-
1141 ing time in hybrid systems: How fast is 'instantaneous'?" in *Proc. IJCAI*,
1142 1995, pp. 1773–1780.
- 1143 [48] B. Heiming and J. Lunze, "Definition of the three-tank benchmark
1144 problem for controller reconfiguration," in *Proc. Eur. Control Conf.*,
AQ7 1145 1999.
- 1146 [49] U. Hanebeck, J. Horn, and G. Schmidh, "On combining statistical and
1147 set-theoretic estimation," *Automatica*, vol. 35, no. 6, pp. 1101–1109,
1148 Jun. 1999.
- 1149 [50] G. Hager, S. Engelson, and S. Atiya, "On comparing statistical and set-
1150 based methods in sensor data fusion," in *Proc. IEEE Int. Conf. Robot.*
1151 *Autom.*, 1993, pp. 352–358.



Emmanuel Benazera received the M.S. degree in 1152 applied mathematics and social sciences from the 1153 University Paris-Dauphine, Paris, France, in 1999 1154 and the Ph.D. degree in computer science from Paul 1155 Sabatier University, Toulouse, France, in 2003. 1156

He was a Visiting Scientist with the NASA 1157 Ames Research Center, Mountain View, CA, for two 1158 years before he joined the Robotics Department, 1159 DFKI/University of Bremen, Bremen, Germany, for 1160 a year. He is currently with LAAS–Centre National 1161 de Recherche Scientifique (CNRS), Université de 1162 Toulouse, Toulouse. His main research interests include automated diagnosis, 1163 decision and planning under uncertainty, and hybrid systems. 1164



Louise Travé-Massuyès (SM'93) received the 1165 Ph.D. degree in control and the Engineering degree 1166 (specialized in control, electronics, and computer 1167 science) from the Institut National des Sciences 1168 Appliquées (INSA), Toulouse, France, in 1984 and 1169 1982, respectively, and the Habilitation Diriger des 1170 Recherches degree from Paul Sabatier University, 1171 Toulouse, in 1998. 1172

She is currently the Research Director of the 1173 Centre National de Recherche Scientifique (CNRS), 1174 LAAS, Toulouse, where she has been the scien- 1175 tific leader of the Diagnosis, Supervision and Control Research Group for 1176 several years. She is responsible for the scientific area of modeling, control, 1177 and system optimization that oversees four research groups in the field of 1178 continuous and discrete automatic control. Her main research interests are in 1179 qualitative and model-based reasoning and applications to dynamic systems 1180 supervision and diagnosis. She has been particularly active in bridging the 1181 AI and control engineering model-based diagnosis communities as the leader 1182 of the BRIDGE Task Group, MONET European Network. She has been 1183 responsible for several industrial and European projects and published more 1184 than 100 papers in international conference proceedings and scientific journals. 1185

Dr. Travé-Massuyès is a Senior Member of the IEEE Computer Society. She 1186 was the recipient of an award from the Union des Groupements d'Ingenieurs de 1187 la Region Midi-Pyrenes. 1188